COVID-19-associated nephropathy includes tubular necrosis and capillary congestion, with evidence of SARS-CoV-2 in the nephron

Antoine Bouquegneau[1, *], Pauline Erpicum[1,2, *], Stéphanie Grosch[1,3, *], Lionel Habran[3], Olivier Hougrand[3], Justine Huart[1,2], Jean-Marie Krzesinski[1,2], Benoît Misset[4], Marie-Pierre Hayette[5], Philippe Delvenne[3], Christophe Bovy[1,3], Dominik Kylies[6], Tobias B. Huber[6], Victor G. Puelles[6], Pierre Delanaye[1,7], Francois Jouret[1,2]

[1]Division of Nephrology, ULiège Academic Hospital (ULiège CHU), Liège, Belgium ;

[2]Groupe Interdisciplinaire de Géno-protéomique Appliquée, Cardiovascular Sciences, ULiège, Liège, Belgium ;

[3]Department of Pathology, ULiège Academic Hospital (ULiège CHU), Liège, Belgium;

[4]Department of Intensive Care, ULiège Academic Hospital (ULiège CHU), Liège, Belgium;

[5]Department of Clinical Microbiology, ULiège Academic Hospital (ULiège CHU), Liège, Belgium;

[6]III. Department of Medicine, University Medical Center Hamburg-Eppendorf, Hamburg, Germany;

[7]Department of Nephrology-Dialysis-Apheresis, University Hospital Caremeau, Nimes, France

Correspondence to: Antoine Bouquegneau; e-mail: antoine.bouquegneau@gmail.com

* These authors all contributed equally to this work.

Key Points

- The pathophysiology of SARS-CoV-2-induced acute kidney injury is poorly understood and may involve direct renal lesions by the virus itself.
- We demonstrated acute tubular necrosis of variable severity, with unusual congestion of the glomerular and peritubular capillaries.
- An immunoreactive signal for SARS-CoV-2 was detected at both RNA and protein levels in various segments of the nephron.

Abstract

Background: Kidney damage has been reported in patients with COVID-19. Despite numerous reports about COVID-19-associated nephropathy, the factual presence of the SARS-CoV-2 in the renal parenchyma remains controversial.

Methods: We consecutively performed 16 immediate (≤3h) *post-mortem* renal biopsies in patients diagnosed with COVID-19. Kidney samples from 5 patients who died from sepsis not related to COVID-19 were used as controls. Samples were methodically evaluated by 3 pathologists. Virus detection in the renal parenchyma was performed in all samples by bulk RNA RT-PCR (E and N1/N2 genes), immunostaining (nCoV2019 N-Protein), fluorescent *in situ* hybridization (nCoV2019-S) and electron microscopy.

Results: The mean age of our COVID-19 cohort was 68.2±12.8 years, most of whom were males (68.7%). Proteinuria was observed in 53.3% of cases, while acute kidney injury occurred in 60% of cases. Acute tubular necrosis of variable severity was found in all cases, with no tubular or interstitial inflammation. There was no difference in acute tubular necrosis severity between the patients with COVID-19 *versus* controls. Congestion in glomerular and peri-tubular capillaries was respectively observed in 56.3 and 87.5% of patients with COVID-19 compared to 20% of controls, with no evidence of thrombi. The nCoV2019 N-Protein was

detected in proximal tubules and also at the basolateral pole of scattered cells of the distal tubules in 9/16 cases. *In situ* hybridization confirmed these findings in 6/16 cases. RT-PCR of kidney total RNA detected SARS-CoV-2 E and N1/N2 genes in one case. Electron microscopy did not show typical viral inclusions.

Conclusions: Our immediate *post-mortem* kidney samples from patients with COVID-19 highlight a congestive pattern of acute kidney injury, with no significant glomerular or interstitial inflammation. Immunostaining and *in situ* hybridization suggest that SARS-CoV-2 is present in various segments of the nephron.

Introduction

A novel coronavirus named SARS-CoV-2 (for "*Severe Acute Respiratory Syndrome Coronavirus 2*") was isolated in December 2019 in China[1]. This virus causes "coronavirus disease 2019" (COVID-19)[1,2], which is characterized by a diffuse alveolar damage leading to an acute respiratory distress syndrome (ARDS)[3,4]. Organs other than the lungs may be affected, including the kidneys[3,5–7]. The earliest report showed that proteinuria and hematuria were detected at hospital admission in 43.9% and 26.7% of patients with COVID-19, while ~15% of them presented with elevated levels of serum creatinine and/or blood urea nitrogen[5]. Proteinuria characterization suggests a tubular origin[8]. Acute kidney injury (AKI) has been identified as an independent risk factor for in-hospital mortality[3–5,9]. In the United States, AKI among hospitalized patients with COVID-19 may range from between 28% and 46%[10], with a high risk of in-hospital mortality[11].

The pathophysiology of COVID-19-associated AKI is poorly understood and may involve (i) the cytokine release syndrome (CRS)[12,13]; (ii) the hypercoagulable state leading to acute tubular necrosis (ATN) and cortical necrosis[14,15]; and/or (iii) direct renal lesions by the virus itself [7,16–18]. In addition, the hemodynamic instability induced by SARS-CoV-2 infection may cause an ischemic ATN *per se*, as typically observed in septic patients. Receptors for SARS-CoV-2 include the angiotensin-converting enzyme 2 (ACE2)[16,19], as well as CD147[20] and GRP78[19]. The ACE2 is largely expressed at the surface of respiratory cells and might be more involved in SARS-CoV-2 infection compared to other receptors. Renal tubular cells and podocytes also express ACE2 on the luminal side of their plasma membrane[21,22]. However, the factual presence of the virus in the urinary system remains largely debated[6,9,23–30].

In the present study, we prospectively aimed (i) to describe the histological findings in consecutive *post-mortem* kidney biopsies of patients with COVID-19 in correlation with their medical history and (ii) to assess whether the SARS-CoV-2 virus is segmentally detectable in the nephron.

Patients and Methods

Patients. Kidney biopsies were performed in adult patients deceased from COVID-19 inside and outside the intensive care unit (ICU) between 30/03/2020 and 04/06/2020 at ULiège Academic Hospital. None of these samples have been used in whole or in part in previous reports. Our study was approved by the Ethics Committee of ULiège Academic Hospital (B707201215598 - 2020/119) in agreement with the ethical standards of Helsinki declaration and the Belgian law about immediate autopsies (which stipulates that autopsies/biopsies may be performed without the written informed consent of the patient or family in case of "urgent medical and/or scientific need", such as a novel infectious disease). Note that relatives of the patients included in the present study were systematically informed before the biopsy procedure. Patients with and without AKI were eligible. The SARS-CoV-2 reverse transcriptase polymerase chain reaction (RT-PCR) was performed on nasopharyngeal swab by using the Cobas® SARS-CoV-2 assay (cobas 6800, Roche) which targets E and ORF1ab genes[31,32]. A control group of 5 patients without COVID-19 was used to more specifically evaluate the COVID-19-induced histological lesions. Four cases with an *ante-mortem* diagnosis of sepsis and/or ARDS, who underwent an autopsy within 24h, were identified in the database of the Department of Pathology (i.e. #R1-R4 patients). One control patient died from pulmonary sepsis not related to COVID-19 in ICU during the present prospective recruitment (#P1 patient) and was PCR-negative for SARS-CoV-2. The immunocompromised status was defined as having a history of cancer or active cancer, transplantation, human immunodeficiency virus infection, type 1 diabetes or inflammatory disease.

Kidney biopsy. Percutaneous kidney biopsy was performed under ultrasound guidance, via a disposable 16-G biopsy needle (ISTOCORE®) targeting the lower pole of the kidney (either left or right). The patient was on prone position. All biopsies were done by the same investigator (AB) within a maximum period of 3 hours *post-mortem*. Three samples (each of ~15mm long

by ~3mm wide) were collected. The first sample was immediately fixed in 10% paraformaldehyde for 48 hours; the second sample was immersed in 4% glutaraldehyde; the third sample was snap-frozen in liquid nitrogen. Conventional protective measures against viral spread were followed, including protection of the airways during the procedures and the fixation of tissue specimens for 48h before handling. The renal paraffin blocks of #R1-R4 control patients were retrieved for the archives and processed in parallel with the COVID-19 samples.

Clinical, biological and radiological parameters. Clinical data was collected from medical records and anonymized: age, weight, height, body mass index (BMI), history of hypertension, history of diabetes, active or previous cancer, active smoking and chronic kidney disease (CKD). All biological data was obtained from the same laboratory. Blood levels of C-reactive protein (CRP), procalcitonin, creatinine, lactate dehydrogenase (LDH) and potassium were determined using the Abbott Alinity instrument. Lymphocytes and platelet measurement were obtained using the Sysmex SE-9000 Hematology analyzer. Plasma D-Dimer levels were measured with the Innovance D-Dimer kit on the automated Siemens CS5100. The number of red blood cells in the urine was automatically evaluated by means of the Sedimax. The estimated glomerular filtration rate (eGFR) was calculated using the chronic kidney disease-epidemiology (CKD-EPI) equation[33]. Proteinuria was staged according to the kidney disease improved global outcomes (KDIGO) staging system[34]. AKI definition and stages were defined according to the KDIGO guidelines[35]. The incidence of a ≥30% decrease of eGFR during hospitalization was also assessed. The severity scoring of COVID-19 pneumonia was based on the percentage of the lungs involved on thorax CT-scanner, as reported by the radiologists in charge: minor if <10 %; mild between 10 and 50 %, and severe if > 50% of lung involvement[36].

Histological analyses.

Light microscopy. All biopsies were prepared using standard techniques. A conventional description by light microscopy based on routine colorations, i.e. Hematoxylin/Eosin (H&E), Periodic Acid Shift (PAS), Jones silver coloration and Masson Trichrome, was performed independently by 3 pathologists (SG, CB, PE) blinded for the medical history, according to an *a priori* defined criteria listed in **Supplementary Table 1**. Briefly, tissue sections were systematically scored for (i) proliferation, sclerosis and ischemia in the glomeruli; (ii) tubulitis, cell vacuolization, necrosis and atrophy in the tubules; (iii) edema, inflammation and fibrosis in the interstitium; and (iv) congestion, thrombi, endothelial cell swelling, arteriolar hyalinosis and peritubular capillaritis in the vasculature[37].

Immunohistochemical studies. Immunohistochemistry was performed on formalin-fixed paraffin-embedded (FFPE) samples. Immunostaining for ACE2 (GeneTex #SN0754), Na^+/Cl^- cotransporter (NCC; rabbit anti-NCC Merck® ab3553), CD10 (VENTANA, #790-4506) and CD31 (VENTANA, #760-4378) was performed on all samples. In cases of erythrocyte aggregation in capillaries, the presence of thrombi was determined using immunohistochemistry for CD61 (platelet marker; Sigma Aldrich), CD42b (platelet marker; BioSB), as well as Martius Blue Scarlet staining (fibrin marker; Atom Scientific #RRSK2-500). The conventional negative and positive controls for each technique were adequately used.

Virus detection. Immunostaining for the nucleocapsid of SARS-CoV-2 was performed on all cases using 2019-nCoV N-Protein (NP) rabbit polyclonal antibody (ABclonal #A20016)[26,38]. Sections of lungs from guinea pigs infected by SARS-CoV-2 were used as positive controls. Briefly, FFPE tissue sections were subjected to H_2O-based antigen retrieval. Endogenous peroxidase activity was blocked with 3% hydrogen peroxide. No-specific binding was constrained by incubation with Protein Block Serum Free. Specimens were then incubated for 60 min at room temperature with primary antibody (1/100). After washing, sections were

incubated for 30 min with Polyview® Plus AP- anti-rabbit secondary antibody (Enzo #ENZ-ACC110-0150). Immunoreactivity was detected using AP (Enzo #ADI-950-I41-0030) and sections were counterstained with H&E. The extent of 2019-nCoV N-Protein positivity was semi-quantitatively scored upon the Banff classification for definitive polyomavirus nephropathy[39]. Total RNA extraction from FFPE kidney sections was performed by the means of Maxwell 16 LEV RNA FFPE kit (Promega AS1260)[40.] RT-PCR was performed on LC480 thermocycler (Roche) using the Viral RNA UM Master Mix (Qiagen) after confirmation of the integrity of the human genetic material (B2M and RNAseP genes). The E and N1/N2 genes of SARS-CoV-2 were targeted using the following cycling conditions: 50°C for 10 min, 95°C for 2 min and 40 cycles at 95°C for 5 sec, 58°C for 30 sec[31].

Fluorescence in situ hybridization (ISH) for SARS-CoV-2 RNA spatial identification. ISH was performed on FFPE human kidney samples using RNAscope®-technology as previously described[41] in accordance with the directions from Advanced Cell Diagnostics. The RNAscope® V-nCoV2019-S probe from Advanced Cell Diagnostics was used as the target probe to detect the SARS-CoV-2 S gene encoding the viral spike protein. Fluorescent labeling of the target probe was performed using OPAL 690 dye from Akoya biosciences (cat. nr. FP1497001KT, dilution 1:1000). RNAscope® 3-plex-positive- and -negative-control probe mix from Advanced Cell Diagnostics were used to ascertain RNA-quality and to exclude false-positive signaling. Fluorescent labeling of the positive- and negative-control probe mix were performed using OPAL 520 and 690 dyes from Akoya biosciences (cat. nr. FP1487001KT, cat. nr. FP1488001KT and cat. nr. FP1497001KT respectively, all dilutions 1:1500). Nuclear co-staining was performed using the DAPI solution from Advanced Cell Diagnostics. Immunostaining with Lotus Tetragonolobus Lectin (LTL) was performed in the same sections after completing the RNAscope-protocol. The primary antibody specific to LTL was applied for 12 hours at 4°C (Vectorlabs; cat. nr. B-1325-2, dilution 1:200). The secondary antibody

Alexa Fluor 555 streptavidin conjugate from Thermo Fischer Scientific (cat. nr. S32355, dilution 1:400) was applied for 60 minutes at 4°C. Epifluorescence imaging was performed using the Thunder Imager 3D Live Cell & 3D Cell Culture from Leica Microsystems.

Electron microscopy. Tissues were fixed at 4°C in 4% glutaraldehyde in phosphate buffer at pH 7.4, post-fixed in 1% osmium tetroxide for 1 hour at 4 °C. Then, they were dehydrated in graded (70%, 90%, 100%) ethanol solutions and propylene oxide, embedded in Epon and hardened at 60 °C. Semi-thin sections were stained with 0.5% toluidine blue and examined by light microscopy. Ultra-thin sections (80 nm) were stained with uranyl acetate and lead citrate. These sections were examined using a Zeiss EM 910 transmission electron microscope (60 kV).

Statistical analyses. Data was expressed as mean [minimum value; maximum value] when the distribution was normal, and as median with interquartile range [quartile1; quartile3] if not. Normality was assessed by the Shapiro-Wilk test. Categorical variables were expressed as percentages. Statistical difference was evaluated by means of a t-test in the case of normally distributed variables or by a rank test where continuous variables were not normally distributed and by means of the Fischer exact test for categorical variables. The Spearman rank-order correlation coefficient was used to measure the strength and direction of association between two variables measured on an ordinal or continuous scale. Analyses were conducted using STATA (version 15; StataCorp, College Station, TX).

Results

Characteristics of the population

All of the 16 Caucasian cases showed a positive RT-PCR-based amplification of SARS-CoV-2 using nasopharyngeal swab before death (basically at hospital admission) and presented with thoracic computerized tomography (CT) compatible with COVID-19 pneumonia. The median length between SARS-CoV-2 positivity through nasopharyngeal sampling and death was 14 days [IQR: 7.5; 25.5]. Their clinical and lab characteristics are summarized in **Table 1**. For informational purposes, **Supplementary Table 2** distinguishes the patients on the basis of their location at the time of death, i.e. inside *versus* outside the ICU. Ten patients (62.5%) died in the ICU. The mean age of our 16-patient cohort was 68.2±12.8 years, with a male predominance (68.7%). ICU patients were significantly younger (p=0.007). The BMI reached 30.7±6.1 kg/m^2. Hypertension, diabetes and CKD were present in 62.5%, 56.3% and 42.9% of cases, respectively (**Table 1**). Our cohort included 2 heart transplant recipients (#7, #11) and 1 patient with a history of prostate cancer (#6). The median length of hospital stay was 14 days [IQR: 7.5; 25.5], with a significantly longer stay for ICU patients (**Supplementary Table 2**). Lymphocyte count was at the lower level of the norm, while blood levels of CRP, fibrinogen, D-dimer and LDH were above the normal ranges at hospital admission (**Table 1 and Supplementary Table 2**). Most of the ICU patients had a more severe form of COVID-19, with a higher prevalence (60%) of severe CT-based score compared to non-ICU patients (16.7%) at admission. AKI concerned 60% of patients during hospitalization, with 53.3% of them showing stage 3 proteinuria at admission with a median proteinuria of 580 [320; 830] mg/g urine creatinine (**Table 1**). During their hospitalization, ICU patients developed a 30%-decrease in eGFR more frequently than non-ICU patients (**Supplementary Table 2**). Three patients required renal replacement therapy (RRT). The clinical and biological characteristics of the control patients (n=5) are summarized in **Supplementary Table 3**. The cause of death was related to sepsis and ARDS in 81.3% of cases.

Histological findings

Table 2 summarizes the most relevant pattern of renal lesions observed by light microscopy in all cases, including both COVID-19 (n=16) and control (n=5) groups. The biopsies had a median of 31 [18; 49] glomeruli, with a median of 12 [2; 17] sclerotic glomeruli in the COVID-19 group. The #P1 sample showed 33 glomeruli with no sclerosis, while the archival #R1-R4 tissues had ≥500 glomeruli. All COVID-19 and control cases demonstrated ATN lesions to a variable extent, which were mainly characterized by tubular vacuolization (n=12/21), loss of proximal tubule (PT) brush border (n=20/21), cell shedding (n=12/21) and/or apoptosis (n=17/21) (**Figure 1**). ATN severity was not different between COVID-19 *versus* control samples. No tubulitis or interstitial infiltrate was observed in either group. In our study, patients (#5, #7, #11) had been exposed to intra-venous (IV) contrast during the hospitalization and 2 patients (#7, #11) were treated by calcineurin inhibitors (CNI) as a long-life therapy for heart transplantation. No patient received IV immunoglobulin, non-steroidal anti-inflammatory drugs or vitamin C during the hospitalization. The intra-tubular hyaline casts were commonly observed (n=13/21). Intra-tubular pigments were detected in 4 patients with COVID-19 (#1, #2, #3 and #9). No viral inclusions or nuclear dystrophies were found. Congestion within glomerular and peri-tubular (PTC) capillaries was respectively observed in 56.3% and 87.5% of cases in the COVID-19 group, whereas only one control patient (#R2) showed PTC aggregation of erythrocytes. Serial staining for CD61 and CD42b evidenced platelets within the congestive PTC in 11/15 cases (including #R2) and within the glomerular capillaries in 7/9 cases (including #R2) (**Supplementary Figure 1**). Fibrin was not found using Martius Blue Scarlett staining. No proliferative glomerular lesions or modifications of the glomerular basement membrane were observed, except for 2 patients with COVID-19 (#12 and #14) with increased mesangial cellularity. One patient with COVID-19 (#8) also showed endocapillary proliferation, with no significant immunoreactive signal for IgA, IgG, IgM, C1q, C4d and C3. Few cases in the COVID-19 group exhibited endothelial cell swelling in the

glomerular capillary loops (#11) or the arterioles (#4). One COVID-19 patient (#6) showed mild intimal arteritis in only one arterial cross-section. Peritubular capillaritis was observed in 3 patients with COVID-19 (#3, #6 and #8) and the control #R1 patient (**Figure 1**). The ACE2 was predominantly located at the brush border of PT cells, as well as at the surface of the parietal epithelial cells of the glomeruli (**Supplementary Figure 2**). No ACE2 staining was noticed in the endothelial cells or the distal tubule (DT). No significant difference in the expression and distribution of ACE2 was observed between COVID-19 *versus* control groups. A significant correlation was found between ATN severity and AKI staging (Spearman correlation = 0.683; p=0.03). No other relevant correlation was obtained between the clinical or biological parameters and histological findings, especially between the KDIGO stage of proteinuria or the *post-mortem* delay of kidney biopsies and PT vacuolization.

Ultrastructural findings

The examination of kidney samples by electron microscopy showed clathrin-coated vesicles characterized by an electron-lucent center (~50 nm in diameter) surrounded by an electron-dense capsule (~100 nm in diameter) in 3 patients (#2, #7, #9) **(Figure 2**). Typically, these particles face the cell cytoplasm and are inside the plasma membrane, which casts doubt on a viral origin[42]. Other ultrastructural features included occasional dense deposits in mesangial or sub-endothelial locations, as well as red blood cell congestion in glomerular capillary loops and PTC **(Figure 2**).

Detection of SARS-CoV-2 in the renal parenchyma using immunostaining against the 2019-nCoV N Protein, in situ hybridization and bulk RNA RT-PCR

Immunostaining for the 2019-nCov N-protein was positive in 9/16 with COVID-19, as simultaneously confirmed by the specific immunoreactive signal observed in lung sections of guinea pigs infected by SARS-CoV-2. Serial sections with markers of PT (CD10), DT (NCC)

and endothelial (CD31) cells revealed a preferential localization of the virus in the cytoplasm of PT cells as well as in the basolateral pole of the cytoplasm of scattered epithelial cells lining the NCC-positive DT (**Figure 3 and Supplementary Figures 3-4**). None of the kidney samples from the control group showed such a dot-shaped signal for the 2019-nCov N-Protein. A faint unspecific immunoreactivity was observed in the cytoplasm of necrotic PT cells in both COVID-19 and control groups. No CD31-positive endothelial cells were positive for the 2019-nCov N-Protein. The extent of tubular positivity for 2019-nCov N-Protein was semi-quantitatively scored (upon a Banff-derived classification[39]) as <1% in 6 patients (#6, #7, #8, #10, #11 and #14), 1-10% in 2 patients (#1 and #9) and >10% of all tubules/ducts in one patient (#3) (**Table 2**). Interestingly enough, the semiquantitative viral load after classical nasopharyngeal sampling had been quantified in 5/16 patients right before death, with a median delay of 2 [1; 3] days. Two patients (#13, #16) had undetectable levels of SARS-CoV-2, whereas 3 patients (#7, #8, #10) showed persistent viral load, with a median cycle threshold (CT) of 27.12 [20.7-31.6] for the E gene of SARS-CoV-2. The immunostaining against 2019-nCov N-Protein on the corresponding kidney samples was negative in patients with undetectable viral load and positive in patients with measurable viral load. The viremia was not available in our series.

A total of 9/16 samples were interpretable by the means of ISH, which contained between 3 and 10 glomeruli (average of 7 glomeruli per specimen). We defined interpretable when we could evaluate the presence or the absence of a signal and when positive (house-keeping) and negative controls (bacterial probe) yielded consistent results. In 7 cases, there were discrepancies between these three factors that would not allow us to make a clear definition. For this reason, the limitations with tissue availability (no chance to repeat the assays in triplicates as required) and the potential confounding effect of autopsy material, we decided to report 9 samples with high level of certainty and the remaining 7 samples as inconclusive. Two samples were positive for nCoV2019-S: #2 (negative by IHC); #4 (negative by IHC). Two

additional samples were considered as borderline positive in glomeruli: #11 (negative by IHC); #9 (negative by IHC). Four samples were considered as borderline positive in the tubular-interstitial compartment: #11 (positive by IHC); #9 (positive by IHC), # 8 (positive by IHC) and #5 (negative by IHC). The remaining 3 ISH-negative samples were positive (#1 and #10) or negative (#15) for the 2019-nCov NP. All of these findings have been summarized in **Table 2**. The ISH signal was detected in scattered cells lining the LTL-positive PT and the LTL-negative peri-glomerular distal tubules, as well as in the glomeruli and the small vessels (**Figure 4 & Supplementary Figure 5**). Positive and negative controls are provided in **Supplementary Figures 6 & 7**.

RT-PCR performed from total RNA extracted from FFPE tissue failed to amplify the E and N1/N2 genes of SARS-CoV-2 in kidney samples, except for one case (#15; CT values of and 32.38 for E and N genes, respectively). The median CT value for human RNAseP gene reached 20.89 [18.39; 26.27] in the whole cohort.

Discussion

COVID-19 is a novel nosological entity, with a broad clinical spectrum. The early description of the entity logically focused on lung involvement, although an increasing number of reports have progressively highlighted the impact of the SARS-CoV-2 on other organs including the kidneys[3,6–8]. Furthermore, correlations between extra-respiratory viral tropism, disease severity, and increased risk of premature death within the first 3 weeks of disease have been highlighted[7]. In our present prospective cohort based on immediate *post-mortem* kidney biopsies, we observed ATN in all cases, with unusual congestion of the glomerular and PTC. No thrombi were factually evidenced. No tubulitis or interstitial inflammation was found. No viral inclusions or nuclear dystrophies were observed. Although SARS-CoV-2 genes could not be consistently detected by the means of RT-PCR of bulk RNA from FFPE kidney samples, a positive signal for SARS-CoV-2 was found at both protein and RNA levels, with a preferential localization in the cytoplasm of both PT and DT cells. SARS-CoV-2 mRNA was also detected in a few glomerular and endothelial cells.

Our findings strengthen the first histological observations highlighting a preferentially tubular pattern of kidney injury, including ATN lesions and PT vacuolization[25,26]. Of important note, endothelial lesions, such as cell swelling with foamy degeneration and subendothelial expansion and proliferation, had been described in this initial report[26]. The hypoxic delay between death and renal sampling may partly explain this pattern of endothelium injury. Examination by electron microscopy showed clusters of particles with distinctive spikes in podocytes and epithelial cells lining the renal tubules. However, these aspects of “virus-like particles” have been strongly challenged since they may correspond to physiological intracellular components like clathrin-coated vesicles and multi-vesicular bodies, as observed in our cohort[27,42,43]. Note that the timing and the location of the kidney biopsy, as well as the expertise of the observer(s), may also influence the yield of EM-based identification of viral particles. The nucleoprotein of SARS-CoV-2 was then found in unspecified renal tubules[25,44].

Another *post-mortem* case-series (with a mean hypoxic delay of 33 hours) demonstrated diffuse ATN, with 3/18 patients showing fibrin thrombi in glomerular capillaries[45]. Thrombosis of the renal microvasculature has also been highlighted in *post-mortem* kidney samples from patients who benefited from extended cardiopulmonary resuscitation (CPR) before death[28]. CPR-associated ischemia may significantly affect the renal microvasculature. In our cohort, all patients died from septic shock or ARDS with no prior CPR. Seventy-five percent of our patients were on anticoagulation therapy during their stay. No thrombotic microangiopathy (TMA) or thrombi within the glomerular capillaries were observed or stained by Martius Blue Scarlett.

Evidence of nephrotic-range proteinuria and collapsing glomerulopathy was reported in patients with COVID-19[29,46]. Diffuse tubule-reticular inclusions called "interferon footprints" were described in glomerular endothelial cells, which may reflect SARS-CoV-2-induced excessive production of interferon[47]. A case-series of 10 COVID-19 patients with AKI and/or proteinuria and/or hematuria showed 2 cases with TMA and 1 case with focal sclerosis and features of healing collapsing glomerulopathy in isolated glomeruli. One patient had pauci-immune crescentic glomerulonephritis. All biopsies were negative for the SARS-CoV-2 NP antigen[48]. A case-series of 17 patients (including 3 kidney transplant recipients) showed various levels of ATN, with no evidence of SARS-CoV-2 (S2 subunit) in the renal parenchyma[37]. Conversely, the spike protein of SARS-CoV-2 was detected in 2/14 patients with COVID-19, as a patchy, granular cytoplasmic staining in tubular epithelial cells[49]. *In situ* hybridization for SARS-CoV-2 was negative in a recent *post-mortem* kidney samples study[50]. Golmai et al. mainly focused on patients with stage 2 or 3 AKI with high rate of patient requiring RRT (n=8/12), whereas with and without AKI were eligible in our study. Note that the delay between death and biopsy in Golmai's report ranges between 1.5 and 70 hours, which may increase the risk of autolysis and biased interpretation of the histological lesions and subsequent technical investigations. Finally, a cohort of 42 autopsies (including 6 patients deceased before hospital

admission) reported on ATN and focal (<5% of glomeruli) fibrin thrombi (n=6 cases). Immunostaining against the spike antigen and *in situ* hybridization for SARS-CoV-2 were negative (n=10 cases)[51]. An important reminder: all of these tissue-based studies necessarily represent a "snapshot" of a highly dynamic pathological process, which may explain the heterogeneous findings regarding the presence of SARS-CoV-2 mRNA and/or protein in the renal parenchyma[44]. Furthermore, the yield of each technique may be impacted by the type of starting materials, such as fresh *versus* snap-frozen *versus* FFPE *versus* RNAlater-preserved samples collected *ante versus post* mortem.

The limitations of our monocentric study include the small number of observations, which prevents us from building robust correlation between the clinical parameters and the histological findings. We have no information about the viremia in our cohort. Of note, positive SARS-CoV-2 viremia has been reported as detectable in less than 40% of patients with COVID-19 pneumonia[52,53]. We provide a detailed clinical and biological description of all cases, thereby allowing correlations and comparisons to previous reports (summarized in **Supplementary Table 4**). As a reminder, patients with or without AKI were eligible in our study, which allowed us to cover an extended spectrum of the COVID-19-associated nephropathy. The *post-mortem* collection of the renal samples may bias the specific identification of renal COVID-19-associated lesions since the features of ATN and *post-mortem* autolysis are very similar. In order to circumvent this limitation, we have included 5 archival kidney samples from patients with septic shock and/or ARDS, and we collected most of the samples within 1-hour after death. Note that 4/5 control tissue specimens were extracted from a historical pathology bank and did not *stricto sensu* follow the same path of harvesting and processing of the COVID-19 tissue samples. All biopsies were methodically described by 3 experienced renal pathologists following *a priori* well-standardized criteria in order to limit the inter-observer variability in the description and scoring of the morphologic features. The severity of the ATN was not different between COVID-19 *versus* control groups. No immune deposits or interstitial

inflammation were found in our series. Conversely, the non-thrombotic congestion in glomerular and peri-tubular capillaries was preferentially observed in patients with COVID-19. Due to the small sample size of the control group, COVID-19-associated capillary congestion must be interpreted with caution. Still, peritubular capillary congestion has been described in other clinical entities, including hantavirus infection (probably secondary to increased endothelial permeability[54]) and renal ischemia/reperfusion[55]. A sepsis-induced decreased of renal perfusion in patients with COVID-19 may also contribute to this histopathological observation. Of important note against the hypothesis of non-specific random morphological *post-mortem* observation, the capillary congestion is not considered as a major criterion of ATN caused by autolysis[56]. Our observations, based both on *in situ* hybridization and immunostaining, support a SARS-CoV-2 kidney tropism in both proximal and distal tubules, despite the absence of definitive ultrastructural evidence. The significance of one single case with positive RT-PCR characterized by a high CT number is questionable. Still, the negative and positive controls of this experiment performed on total RNA extracted from FFPE tissue were repeatedly concordant with the detection of SARS-CoV-2 E & N genes in the renal bulk RNA of this patient.

In conclusion, our collection of immediate *post-mortem* kidney biopsies highlights a congestive pattern of COVID-19-associated AKI, with SARS-CoV-2 detection in various segment of the nephron.

Disclosures: P. Delanaye reports Consultancy Agreements: Immunodiagnostic Systems limited, ARK Biosciences; Honoraria: Sanofi, Bayer, AstraZeneca, Amgen, Menarini, Siemens, Fresenius. T. Huber reports Consultancy Agreements: AstraZeneca, Bayer, Boehringer-Ingelheim, DaVita, Deerfield, Fresenius Medical Care, GoldfinchBio, Mantrabio, Novartis, and Retrophin Research Funding: Amicus Therapeutics, Fresenius Medical Care; Scientific Advisor or Membership: Kidney International (Journal; Editorial board), Nature Review Nephrology (Journal, Advisory Board). F. Jouret reports Consultancy Agreements: ORGENESIS; Honoraria: AMGEN, OTSUKA; Scientific Advisor or Membership: Belgian Society of Nephrology. J. Krzesinski reports Consultancy Agreements: Bayer, Boehringer, Vifor pharma, Menarini; Honoraria: Bayer, Menarini, Vifor, Boehringer. All remaining authors have nothing to disclose.

Funding: ULiege Fondation Leon Fredericq; Fonds National de la Recherche Scientifique

Acknowledgements: We sincerely thank all physicians and nurses who take care of COVID-19 patients in the clinical wards and intensive care units. We also thank all members of the department of Medico-Economic Information Service (SIMÉ), as well as Laurence Poma (ULiège GIGA Cardiovascular Sciences), François Maclot (ULiège CHU, Department of Clinical Microbiology) and Michael Sarlet (ULiège, School of Veterinary Medicine) for their technical assistance. Our manuscript has been reviewed by a native speaker: Enda Breen (enda.breen4@mail.dcu.ie), who is a member of the Irish Translators' and Interpreters' Association (ITIA). PE, JH and FJ are Fellows of the Fonds National de la Recherche Scientifique (FNRS), Brussels, Belgium.

Author contributions: A Bouquegneau: Conceptualization; Data curation; Formal analysis; Investigation; Methodology; Validation; Visualization; Writing - original draft; Writing - review and editing

P Erpicum: Data curation; Formal analysis; Investigation; Methodology; Validation; Writing - original draft; Writing - review and editing

S Grosch: Data curation; Methodology; Validation; Writing - review and editing

L Habran: Formal analysis; Methodology; Writing - review and editing

O Hougrand: Formal analysis; Methodology; Writing - review and editing

J Huart: Formal analysis; Validation; Writing - review and editing

J-M Krzesinski: Conceptualization; Writing - review and editing

B Misset: Conceptualization; Writing - review and editing

M-P Hayette: Formal analysis; Validation; Writing - review and editing

P Delvenne: Conceptualization; Validation; Writing - review and editing

C Bovy: Formal analysis; Methodology; Validation; Writing - review and editing

D Kylies: Formal analysis; Methodology; Writing - review and editing

T Huber: Formal analysis; Writing - review and editing

V Puelles: Formal analysis; Methodology; Validation; Writing - review and editing

P Delanaye: Conceptualization; Formal analysis; Methodology; Supervision; Validation; Visualization; Writing - original draft; Writing - review and editing

F Jouret: Conceptualization; Formal analysis; Methodology; Supervision; Validation; Visualization; Writing - original draft; Writing - review and editing

All authors reviewed and approved the final version of the manuscript.

Supplemental material Table of Contents

References

1. Zhu N, Zhang D, Wang W, Li X, Yang B, Song J, Zhao X, Huang B, Shi W, Lu R, Niu P, Zhan F, Ma X, Wang D, Xu W, Wu G, Gao GF, Tan W, China Novel Coronavirus Investigating and Research Team: A Novel Coronavirus from Patients with Pneumonia in China, 2019. *N. Engl. J. Med.* 382: 727–733, 2020

2. Li Q, Guan X, Wu P, Wang X, Zhou L, Tong Y, Ren R, Leung KSM, Lau EHY, Wong JY, Xing X, Xiang N, Wu Y, Li C, Chen Q, Li D, Liu T, Zhao J, Liu M, Tu W, Chen C, Jin L, Yang R, Wang Q, Zhou S, Wang R, Liu H, Luo Y, Liu Y, Shao G, Li H, Tao Z, Yang Y, Deng Z, Liu B, Ma Z, Zhang Y, Shi G, Lam TTY, Wu JT, Gao GF, Cowling BJ, Yang B, Leung GM, Feng Z: Early Transmission Dynamics in Wuhan, China, of Novel Coronavirus-Infected Pneumonia. *N. Engl. J. Med.* 382: 1199–1207, 2020

3. Huang C, Wang Y, Li X, Ren L, Zhao J, Hu Y, Zhang L, Fan G, Xu J, Gu X, Cheng Z, Yu T, Xia J, Wei Y, Wu W, Xie X, Yin W, Li H, Liu M, Xiao Y, Gao H, Guo L, Xie J, Wang G, Jiang R, Gao Z, Jin Q, Wang J, Cao B: Clinical features of patients infected with 2019 novel coronavirus in Wuhan, China. *Lancet* 395: 497–506, 2020

4. Guan W-J, Ni Z-Y, Hu Y, Liang W-H, Ou C-Q, He J-X, Liu L, Shan H, Lei C-L, Hui DSC, Du B, Li L-J, Zeng G, Yuen K-Y, Chen R-C, Tang C-L, Wang T, Chen P-Y, Xiang J, Li S-Y, Wang J-L, Liang Z-J, Peng Y-X, Wei L, Liu Y, Hu Y-H, Peng P, Wang J-M, Liu J-Y, Chen Z, Li G, Zheng Z-J, Qiu S-Q, Luo J, Ye C-J, Zhu S-Y, Zhong N-S, China Medical Treatment Expert Group for Covid-19: Clinical Characteristics of Coronavirus Disease 2019 in China. *N. Engl. J. Med.* 382: 1708–1720, 2020

5. Cheng Y, Luo R, Wang K, Zhang M, Wang Z, Dong L, Li J, Yao Y, Ge S, Xu G: Kidney disease is associated with in-hospital death of patients with COVID-19. *Kidney Int.* 97: 829–838, 2020

6. Puelles VG, Lütgehetmann M, Lindenmeyer MT, Sperhake JP, Wong MN, Allweiss L, Chilla S, Heinemann A, Wanner N, Liu S, Braun F, Lu S, Pfefferle S, Schröder AS, Edler C, Gross O, Glatzel M, Wichmann D, Wiech T, Kluge S, Pueschel K, Aepfelbacher M, Huber TB: Multiorgan and Renal Tropism of SARS-CoV-2. *N. Engl. J. Med.* 383: 590–592, 2020

7. Braun F, Lütgehetmann M, Pfefferle S, Wong MN, Carsten A, Lindenmeyer MT, Nörz D, Heinrich F, Meißner K, Wichmann D, Kluge S, Gross O, Pueschel K, Schröder AS, Edler C, Aepfelbacher M, Puelles VG, Huber TB: SARS-CoV-2 renal tropism associates with acute kidney injury. *Lancet* 396: 597–598, 2020

8. Huart J, Bouquegneau A, Lutteri L, Erpicum P, Grosch S, Résimont G, Wiesen P, Bovy C, Krzesinski J-M, Thys M, Lambermont B, Misset B, Pottel H, Mariat C, Cavalier E, Burtey S, Jouret F, Delanaye P: Proteinuria in COVID-19: prevalence, characterization and prognostic role. *J. Nephrol.* 2021

9. Wang W, Xu Y, Gao R, Lu R, Han K, Wu G, Tan W: Detection of SARS-CoV-2 in Different Types of Clinical Specimens. *J. Am. Med. Assoc.* 323: 1843–1844, 2020

10. Hirsch JS, Ng JH, Ross DW, Sharma P, Shah HH, Barnett RL, Hazzan AD, Fishbane S, Jhaveri KD, Northwell COVID-19 Research Consortium, Northwell Nephrology

COVID-19 Research Consortium: Acute kidney injury in patients hospitalized with COVID-19. *Kidney Int.* 98: 209–218, 2020

11. Ng JH, Hirsch JS, Hazzan A, Wanchoo R, Shah HH, Malieckal DA, Ross DW, Sharma P, Sakhiya V, Fishbane S, Jhaveri KD, Northwell Nephrology COVID-19 Research Consortium Members: Outcomes Among Patients Hospitalized With COVID-19 and Acute Kidney Injury. *Am. J. Kidney Dis.* S0272-6386: 30998–7, 2020

12. Pedersen SF, Ho Y-C: SARS-CoV-2: a storm is raging. *J. Clin. Invest.* 130: 2202–2205, 2020

13. Mehta P, McAuley DF, Brown M, Sanchez E, Tattersall RS, Manson JJ, HLH Across Speciality Collaboration, UK: COVID-19: consider cytokine storm syndromes and immunosuppression. *Lancet* 395: 1033–1034, 2020

14. Tang N, Li D, Wang X, Sun Z: Abnormal coagulation parameters are associated with poor prognosis in patients with novel coronavirus pneumonia. *J. Thromb. Haemost.* 18: 844–847, 2020

15. Zhang Y, Xiao M, Zhang S, Xia P, Cao W, Jiang W, Chen H, Ding X, Zhao H, Zhang H, Wang C, Zhao J, Sun X, Tian R, Wu W, Wu D, Ma J, Chen Y, Zhang D, Xie J, Yan X, Zhou X, Liu Z, Wang J, Du B, Qin Y, Gao P, Qin X, Xu Y, Zhang W, Li T, Zhang F, Zhao Y, Li Y, Zhang S: Coagulopathy and Antiphospholipid Antibodies in Patients with Covid-19. *N. Engl. J. Med.* 382: e38, 2020

16. Hamming I, Timens W, Bulthuis MLC, Lely AT, Navis GJ, van Goor H: Tissue distribution of ACE2 protein, the functional receptor for SARS coronavirus. A first step in understanding SARS pathogenesis. *J. Pathol.* 203: 631–637, 2004

17. Ye M, Wysocki J, William J, Soler MJ, Cokic I, Batlle D: Glomerular localization and expression of Angiotensin-converting enzyme 2 and Angiotensin-converting enzyme: implications for albuminuria in diabetes. *J. Am. Soc. Nephrol.* 17: 3067–3075, 2006

18. Kormann R, Jacquot A, Alla A, Corbel A, Koszutski M, Voirin P, Garcia Parrilla M, Bevilacqua S, Schvoerer E, Gueant J-L, Namour F, Levy B, Frimat L, Oussalah A: Coronavirus disease 2019: acute Fanconi syndrome precedes acute kidney injury. *Clin. Kidney J.* 13: 362–370, 2020

19. Aguiar JA, Tremblay BJ-M, Mansfield MJ, Woody O, Lobb B, Banerjee A, Chandiramohan A, Tiessen N, Cao Q, Dvorkin-Gheva A, Revill S, Miller MS, Carlsten C, Organ L, Joseph C, John A, Hanson P, Austin RC, McManus BM, Jenkins G, Mossman K, Ask K, Doxey AC, Hirota JA: Gene expression and in situ protein profiling of candidate SARS-CoV-2 receptors in human airway epithelial cells and lung tissue. *Eur. Respir. J.* 56: 2001123, 2020

20. Su H, Wan C, Wang Z-D, Gao Y, Li Y-C, Tang F, Zhu H-Y, Yi L-X, Zhang C: Expression of CD147 and Cyclophilin A in Kidneys of Patients with COVID-19. *Clin. J. Am. Soc. Nephrol.* [Internet] CJN.09440620: 2020 Available from: https://cjasn.asnjournals.org/content/early/2020/12/02/CJN.09440620 [cited 2020 Dec 3]

21. Lely AT, Hamming I, van Goor H, Navis GJ: Renal ACE2 expression in human kidney disease. *J. Pathol.* 204: 587–593, 2004

22. Soler MJ, Ye M, Wysocki J, William J, Lloveras J, Batlle D: Localization of ACE2 in the renal vasculature: amplification by angiotensin II type 1 receptor blockade using telmisartan. *Am. J. Physiol. Renal Physiol.* 296: F398-405, 2009

23. Peng L, Liu J, Xu W, Luo Q, Chen D, Lei Z, Huang Z, Li X, Deng K, Lin B, Gao Z: SARS-CoV-2 can be detected in urine, blood, anal swabs, and oropharyngeal swabs specimens. *J. Med. Virol.* 92: 1676–1680, 2020

24. Wölfel R, Corman VM, Guggemos W, Seilmaier M, Zange S, Müller MA, Niemeyer D, Jones TC, Vollmar P, Rothe C, Hoelscher M, Bleicker T, Brünink S, Schneider J, Ehmann R, Zwirglmaier K, Drosten C, Wendtner C: Virological assessment of hospitalized patients with COVID-2019. *Nature* 581: 465–469, 2020

25. Diao B, Wang C, Wang R, Feng Z, Tan Y, Wang H, Wang C, Liu L, Liu Y, Liu Y, Wang G, Yuan Z, Ren L, Wu Y, Chen Y: Human Kidney is a Target for Novel Severe Acute Respiratory Syndrome Coronavirus 2 (SARS-CoV-2) Infection | medRxiv [Internet]. Available from: https://www.medrxiv.org/content/10.1101/2020.03.04.20031120v4 [cited 2020 Dec 9]

26. Su H, Yang M, Wan C, Yi L-X, Tang F, Zhu H-Y, Yi F, Yang H-C, Fogo AB, Nie X, Zhang C: Renal histopathological analysis of 26 postmortem findings of patients with COVID-19 in China. *Kidney Int.* 98: 219–227, 2020

27. Farkash EA, Wilson AM, Jentzen JM: Ultrastructural Evidence for Direct Renal Infection with SARS-CoV-2. *J. Am. Soc. Nephrol.* 31: 1683–1687, 2020

28. Rapkiewicz AV, Mai X, Carsons SE, Pittaluga S, Kleiner DE, Berger JS, Thomas S, Adler NM, Charytan DM, Gasmi B, Hochman JS, Reynolds HR: Megakaryocytes and platelet-fibrin thrombi characterize multi-organ thrombosis at autopsy in COVID-19: A case series. *EClinicalMedicine* 24: 100434, 2020

29. Wu H, Larsen CP, Hernandez-Arroyo CF, Mohamed MMB, Caza T, Sharshir M, Chughtai A, Xie L, Gimenez JM, Sandow TA, Lusco MA, Yang H, Acheampong E, Rosales IA, Colvin RB, Fogo AB, Velez JCQ: AKI and Collapsing Glomerulopathy Associated with COVID-19 and APOL1 High-Risk Genotype. *J. Am. Soc. Nephrol.* 31: 1688–1695, 2020

30. Wichmann D, Sperhake J-P, Lütgehetmann M, Steurer S, Edler C, Heinemann A, Heinrich F, Mushumba H, Kniep I, Schröder AS, Burdelski C, de Heer G, Nierhaus A, Frings D, Pfefferle S, Becker H, Bredereke-Wiedling H, de Weerth A, Paschen H-R, Sheikhzadeh-Eggers S, Stang A, Schmiedel S, Bokemeyer C, Addo MM, Aepfelbacher M, Püschel K, Kluge S: Autopsy Findings and Venous Thromboembolism in Patients With COVID-19: A Prospective Cohort Study. *Ann. Intern. Med.* 173: 268–277, 2020

31. Corman VM, Landt O, Kaiser M, Molenkamp R, Meijer A, Chu DK, Bleicker T, Brünink S, Schneider J, Schmidt ML, Mulders DG, Haagmans BL, van der Veer B, van den Brink S, Wijsman L, Goderski G, Romette J-L, Ellis J, Zambon M, Peiris M, Goossens H, Reusken C, Koopmans MP, Drosten C: Detection of 2019 novel coronavirus (2019-nCoV) by real-time RT-PCR. *Euro Surveill.* 25: 2000045, 2020

32. Artesi M, Bontems S, Göbbels P, Franckh M, Maes P, Boreux R, Meex C, Melin P, Hayette M-P, Bours V, Durkin K: A Recurrent Mutation at Position 26340 of SARS-CoV-2 Is Associated with Failure of the E Gene Quantitative Reverse Transcription-PCR Utilized in a Commercial Dual-Target Diagnostic Assay. *J. Clin. Microbiol.* 58: e01598-20, 2020

33. Matsushita K, Mahmoodi BK, Woodward M, Emberson JR, Jafar TH, Jee SH, Polkinghorne KR, Shankar A, Smith DH, Tonelli M, Warnock DG, Wen C-P, Coresh J, Gansevoort RT, Hemmelgarn BR, Levey AS, Chronic Kidney Disease Prognosis Consortium: Comparison of risk prediction using the CKD-EPI equation and the MDRD study equation for estimated glomerular filtration rate. *J Am Med Assoc* 307: 1941–1951, 2012

34. Kidney Disease: Improving Global Outcomes (KDIGO) CKD Work Group. KDIGO clinical practice guideline for the evaluation and management of chronic kidney disease. *Kidney Int Suppl.* 3: 1–150, 2013

35. Kellum JA, Lameire N, KDIGO AKI Guideline Work Group: Diagnosis, evaluation, and management of acute kidney injury: a KDIGO summary (Part 1). *Crit. Care* 17: 204, 2013

36. Chung M, Bernheim A, Mei X, Zhang N, Huang M, Zeng X, Cui J, Xu W, Yang Y, Fayad ZA, Jacobi A, Li K, Li S, Shan H: CT Imaging Features of 2019 Novel Coronavirus (2019-nCoV). *Radiology* 295: 202–207, 2020

37. Kudose S, Hoshi M, Jain S, Gaut JP: Renal Histopathologic Findings Associated With Severity of Clinical Acute Kidney Injury. *Am. J. Surg. Pathol.* 42: 625–635, 2018

38. Liu J, Babka AM, Kearney BJ, Radoshitzky SR, Kuhn JH, Zeng X: Molecular detection of SARS-CoV-2 in formalin-fixed, paraffin-embedded specimens. *JCI Insight* 5: e139042, 2020

39. Nickeleit V, Singh HK, Randhawa P, Drachenberg CB, Bhatnagar R, Bracamonte E, Chang A, Chon WJ, Dadhania D, Davis VG, Hopfer H, Mihatsch MJ, Papadimitriou JC, Schaub S, Stokes MB, Tungekar MF, Seshan SV, Banff Working Group on Polyomavirus Nephropathy: The Banff Working Group Classification of Definitive Polyomavirus Nephropathy: Morphologic Definitions and Clinical Correlations. *J. Am. Soc. Nephrol.* 29: 680–693, 2018

40. Bonin S, Hlubek F, Benhattar J, Denkert C, Dietel M, Fernandez PL, Höfler G, Kothmaier H, Kruslin B, Mazzanti CM, Perren A, Popper H, Scarpa A, Soares P, Stanta G, Groenen PJTA: Multicentre validation study of nucleic acids extraction from FFPE tissues. *Virchows Arch. Int. J. Pathol.* 457: 309–317, 2010

41. Wang F, Flanagan J, Su N, Wang L-C, Bui S, Nielson A, Wu X, Vo H-T, Ma X-J, Luo Y: RNAscope: a novel in situ RNA analysis platform for formalin-fixed, paraffin-embedded tissues. *J. Mol. Diagn.* 14: 22–29, 2012

42. Miller SE, Brealey JK: Visualization of putative coronavirus in kidney. *Kidney Int.* 98: 231–232, 2020

43. Frelih M, Erman A, Wechtersbach K, Pleško J, Avšič-Županc T, Kojc N: SARS-CoV-2 Virions or Ubiquitous Cell Structures? Actual Dilemma in COVID-19 Era. *Kidney Int. Rep.* 5: 1608–1610, 2020

44. Müller JA, Groß R, Conzelmann C, Krüger J, Merle U, Steinhart J, Weil T, Koepke L, Bozzo CP, Read C, Fois G, Eiseler T, Gehrmann J, van Vuuren J, Wessbecher IM, Frick M, Costa IG, Breunig M, Grüner B, Peters L, Schuster M, Liebau S, Seufferlein T, Stenger S, Stenzinger A, MacDonald PE, Kirchhoff F, Sparrer KMJ, Walther P, Lickert H, Barth TFE, Wagner M, Münch J, Heller S, Kleger A: SARS-CoV-2 infects and replicates in cells of the human endocrine and exocrine pancreas. *Nat. Metab.* 2021

45. Menter T, Haslbauer JD, Nienhold R, Savic S, Hopfer H, Deigendesch N, Frank S, Turek D, Willi N, Pargger H, Bassetti S, Leuppi JD, Cathomas G, Tolnay M, Mertz KD, Tzankov A: Postmortem examination of COVID-19 patients reveals diffuse alveolar damage with severe capillary congestion and variegated findings in lungs and other organs suggesting vascular dysfunction. *Histopathology* 77: 198–209, 2020

46. Shetty AA, Tawhari I, Safar-Boueri L, Seif N, Alahmadi A, Gargiulo R, Aggarwal V, Usman I, Kisselev S, Gharavi AG, Kanwar Y, Quaggin SE: COVID-19-Associated Glomerular Disease. *J. Am. Soc. Nephrol.* 2020

47. Hadjadj J, Yatim N, Barnabei L, Corneau A, Boussier J, Smith N, Péré H, Charbit B, Bondet V, Chenevier-Gobeaux C, Breillat P, Carlier N, Gauzit R, Morbieu C, Pène F, Marin N, Roche N, Szwebel T-A, Merkling SH, Treluyer J-M, Veyer D, Mouthon L, Blanc C, Tharaux P-L, Rozenberg F, Fischer A, Duffy D, Rieux-Laucat F, Kernéis S, Terrier B: Impaired type I interferon activity and inflammatory responses in severe COVID-19 patients. *Science* 369: 718–724, 2020

48. Sharma P, Uppal NN, Wanchoo R, Shah HH, Yang Y, Parikh R, Khanin Y, Madireddy V, Larsen CP, Jhaveri KD, Bijol V, Northwell Nephrology COVID-19 Research Consortium: COVID-19-Associated Kidney Injury: A Case Series of Kidney Biopsy Findings. *J. Am. Soc. Nephrol.* 31: 1948–1958, 2020

49. Bradley BT, Maioli H, Johnston R, Chaudhry I, Fink SL, Xu H, Najafian B, Deutsch G, Lacy JM, Williams T, Yarid N, Marshall DA: Histopathology and ultrastructural findings of fatal COVID-19 infections in Washington State: a case series. *Lancet* 396: 320–332, 2020

50. Golmai P, Larsen CP, DeVita MV, Wahl SJ, Weins A, Rennke HG, Bijol V, Rosenstock JL: Histopathologic and Ultrastructural Findings in Postmortem Kidney Biopsy Material in 12 Patients with AKI and COVID-19. *J. Am. Soc. Nephrol.* 31: 1944–1947, 2020

51. Santoriello D, Khairallah P, Bomback AS, Xu K, Kudose S, Batal I, Barasch J, Radhakrishnan J, D'Agati V, Markowitz G: Postmortem Kidney Pathology Findings in Patients with COVID-19. *J. Am. Soc. Nephrol.* 31: 2158–2167, 2020

52. Sun J, Tang X, Bai R, Liang C, Zeng L, Lin H, Yuan R, Zhou P, Huang X, Xiong Q, Peng J, Cui F, Ke B, Su J, Liu Z, Lu J, Tian J, Sun R, Ke C: The kinetics of viral load and antibodies to SARS-CoV-2. *Clin. Microbiol. Infect.* 26: 1690.e1-1690.e4, 2020

53. Chen X, Zhao B, Qu Y, Chen Y, Xiong J, Feng Y, Men D, Huang Q, Liu Y, Yang B, Ding J, Li F: Detectable Serum Severe Acute Respiratory Syndrome Coronavirus 2 Viral Load (RNAemia) Is Closely Correlated With Drastically Elevated Interleukin 6 Level in Critically Ill Patients With Coronavirus Disease 2019. *Clin. Infect. Dis.* 71: 1937–1942, 2020

54. Muranyi W, Bahr U, Zeier M, van der Woude FJ: Hantavirus infection. *J. Am. Soc. Nephrol.* 16: 3669–3679, 2005

55. Ysebaert DK, De Greef KE, De Beuf A, Van Rompay AR, Vercauteren S, Persy VP, De Broe ME: T cells as mediators in renal ischemia/reperfusion injury. *Kidney Int.* 66: 491–496, 2004

56. Kocovski L, Duflou J: Can renal acute tubular necrosis be differentiated from autolysis at autopsy? *J. Forensic Sci.* 54: 439–442, 2009

57. Roufosse C, Simmonds N, Clahsen-van Groningen M, Haas M, Henriksen KJ, Horsfield C, Loupy A, Mengel M, Perkowska-Ptasińska A, Rabant M, Racusen LC, Solez K, Becker JU: A 2018 Reference Guide to the Banff Classification of Renal Allograft Pathology. *Transplantation* 102: 1795–1814, 2018

Table 1. Clinical and biological characteristics of the SARS-CoV-2 infected group

CLINICAL	
Age (years) – mean [min; max] (n=16)	68.2 [49; 95]
Women – % (n=16)	31.3
Body Mass index (kg/m²) – mean [min; max] (n=16)	30.7 [20.7; 39.6]
Medical history	
Hypertension – % (n=16)	62.5
Diabetes – % (n=16)	56.3
Chronic kidney disease – % (n=14)	42.9
Active cancer or history – % (n=14)	12.5
Cardiovascular disease – % (n=16)	43.8
Immunocompromise status – % (n=16)	25
Asthma/COPD – % (n=16)	0
Non-smoker – % (n=14)	78.6
RAAS inhibitors drugs – % (n=16)	50
Hydroxychloroquine used during hospitalization – % (n=16)	87.5
Contrast products injection during hospitalization – % (n=16)	18.8
Anti-platelets used priori hospitalization – % (n=16)	43.8
Anticoagulation during hospitalization – % (n=16)	75
Hospital stay length (days) – median [IQR] (n=16)	14 [7.5; 22.5]
Severity	
ICU admission – % (n=16)	62.5
Thorax CT-Scanner staging – % (n=16)	
Minor (<10%)	18.8
Mild (10-50%)	37.5
Severe (>50%)	43.7
Renal severity	
AKI – % (n=16)	62.5
CVVH initiation during hospitalization – % (n=16)	18.5
30% decrease of eGFR during hospitalization – % (n=16)	50
Proteinuria at D0 > 500 mg/g of urine creatinine – % (n=15)	53.3
Hematuria at D0 – % (n=13)	53.8

BIOLOGICAL	
ABO group – % (n=14) A – B – AB – O	 64.3 – 14.3 – 0 –21.4
Lymphocytes at D0 (/mm³) – median [IQR] (n=16) Lymphocytes at end of hospitalization (/mm³) – median [IQR] (n=15)	720 [520; 1440] 970 [530; 1280] †
Platelet at D0 (x1000/mm³) – mean [min; max] (n=16) Platelet at end of hospitalization (x1000/mm³) – mean [min; max] (n=15)	211.4 [79; 417] 230.3 [26; 457] †
C-reactive protein at D0 (mg/L) – mean [min; max] (n=16) C-reactive protein at end of hospitalization (mg/L) – mean [min; max] (n=15)	166.5 [4.4; 382.4] 195.5 [3.8; 311.9] †
Fibrinogen (g/L) at D0 – median [IQR] (n=16) Fibrinogen (g/L) at end of hospitalization – median [IQR] (n=15)	7.18 [4.83; 7.72] 6.96 [5.01; 7.86] †
Procalcitonin at D0 (µg/L) – median [IQR] (n=13)	0.33 [0.16; 0.83]
D-Dimer at D0 (µg/L) – mean [min; max] (n=11)	1309.5 [329; 2991]
LDH at D0 (U/L) – mean [min; max] (n=16)	532.8 [195; 881]
CPK at D0 (U/L) – median [IQR] (n=16)	286.5 [181.5; 445]
eGFR (prior the hospitalization) (n=13) 60-90mL/min/1,73m^2 – % < 60mL/min/1,73m^2 – % < 30 mL/min/1,73m^2 – % Serum creatinine at D0 (mg/dL) – median [IQR] (n=16) Serum creatinine at end of hospitalization (mg/dL) – median [IQR] (n=16)	 46.2 23.1 0 1.07 [0.83; 1.27] 0.96 [0.68; 1.62] †
Potassium at D0 (mmol/L) – mean [min; max] (n=16)	4.16 [3.55; 4.63]
Proteinuria at D0 (mg/g of urine creatinine) – median [IQR] (n=15) Proteinuria at D7 (mg/g of urine creatinine) – median [IQR] (n=10)	580 [320; 830] 650 [400; 1520] ‡
Delay Biopsy (n=16) **< 60 (min) – %** **60-120 (min) – %** **120-180 (min) – %**	 62.5 12.5 25

AKI: acute kidney injury; COPD: chronic obstructive pulmonary disease; CPK: creatinine phospho-kinase; CVVH: continuous veno-venous hemofiltration; eGFR: estimated glomerular filtration rate; ICU: intensive care unit; IQR: interquartile range; LDH: lactate dehydrogenase; RAAS: renin angiotensin aldosterone system; SARS-CoV-2: severe acute respiratory syndrome coronavirus 2; SD: standard deviation

† no statistical difference observed between D0 and the end of hospitalization

‡ no statistical difference observed between D0 and D7

Table 2. Clinical data and most relevant acute renal lesions observed by light microscopy, immunostaining, *in situ* hybridization

			GLOMERULI			TUBULO-INTERSTITIUM			PTC		SARS-COV-2			CLINICAL DATA			
						Acute Tubular Necrosis					IHC	ISH					
		Patient ID	Ischemia	Capillary congestion	Endothelial cell swelling	Severity	Extent	Tubular vacuolization	Capillaritis	Congestion	Tubules	Glomeruli	Tubules	DM	HTN	AKI stage	Proteinuria mg/g
COVID	ICU	**3**	N	Y	N	Mild	>0-25%	N	ptc1	Y	>10%	NA	NA	N	Y	2	333
		4	Y	Y	N	Mild	>0-25%	>0-25%	ptc0	Y	N	Y	Y	Y	N	N	595
		6	Y	Y	N	Mild	26-50%	N	ptc1	Y	<1%	NA	NA	N	Y	2	453
		7	Y	N	N	Severe	>50%	>0-25%*°	ptc0	Y	<1%	NA	NA	N	Y	RRT	353
		8	N	N	N	Severe	>50%	N	ptc2	Y	<1%	N	Bdl	N	N	RRT	689
		10	N	N	N	Severe	>50%	N	ptc0	Y	<1%	N	N	Y	Y	RRT	317
		11	N	Y	Y	Mild	26-50%	26-50%*°	ptc0	Y	<1%	Bdl	Bdl	N	N	1	230
		13	N	Y	N	Mild	>0-25%	>0-25%	ptc0	Y	N	NA	NA	Y	Y	3	834
		15	N	Y	N	Moderate	>50%	>0-25%	ptc0	N	N	N	N	N	Y	2	728
		16	N	N	N	Mild	>50%	N	ptc0	Y	N	NA	NA	Y	N	N	1484
	NON-ICU	**1**	Y	Y	N	Mild	>0-25%	N	ptc0	Y	1-10%	N	N	Y	N	N	NA
		2	N	N	N	Mild	>0-25%	N	ptc0	Y	N	Y	Y	Y	Y	N	303
		5	N	N	N	Mild	>0-25%	>0-25%*	ptc0	Y	N	N	Bdl	Y	N	N	1104
		9	N	Y	N	Mild	>0-25%	>0-25%	ptc0	Y	1-10%	Bdl	Bdl	Y	Y	N	268
		12	Y	N	N	Mild	>0-25%	26-50%	ptc0	Y	N	NA	NA	Y	Y	2	6004
		14	N	Y	N	Mild	26-50%	>0-25%	ptc0	N	<1%	NA	NA	N	Y	1	579
CONTROL	ICU	**P1**	N	N	Y	Mild	26-50%	N*	ptc0	N	N			N	N	1	654
		R1	Y	N	N	Severe	>50%	>50%	ptc2	N	N			N	Y	3	387
		R2	N	N	N	Severe	>50%	N*	ptc0	Y	N			Y	N	2	2607
		R3	N	N	N	Moderate	>50%	>0-25%*	ptc0	N	N			Y	Y	RRT	NA
		R4	N	N	N	Severe	>50%	26-50%	ptc0	N	N			N	N	2	NA

AKI: acute kidney injury; bdl; borderline; pct: peritubular capillaries; DM: diabetes mellitus ID: identification number; HTN: hypertension; ICU: intensive care unit; IHC: immunohistochemistry; ISH: *in situ* hybridation; N: not detected; NA: not available; RRT: renal replacement therapy; Y: detected. P= proteinuria expressed in mg/g of urine creatinine. *Patients exposed to IV contrast; °Patients treated by calcineurin inhibitor.
Capillaritis was scored according to the *Banff* scoring system (0: <10% cortical PTC containing leukocytes ;1: ≥ 10% cortical PTC containing 3-4 leukocytes; 2: ≥ 10% cortical PTC containing 5-10 leukocytes)[57]

Legends

Figure 1. Representative histological findings in *post-mortem* kidney biopsies from patients with COVID-19

(A) Acute tubular necrosis with thinning of the tubular epithelium, loss of brush border and cell shedding (PAS staining, patient #7) ; **(B)** Cytoplasmic vacuolization (arrow) of proximal tubular epithelial cells (PAS staining, patient #14); **(C)** Intimal arteritis (arrow; Hematoxylin & Eosine coloration, patient #6); **(D)** Peritubular capillaritis (*) and congestion in peritubular capillaries (+); Jones, patient #3 **(E)** Glomerular endothelial cell swelling and congestion in peritubular capillaries (+; PAS staining, patient #11) **(F)** Congestion in glomerular capillaries (arrow; PAS staining, patient #6). *Scale bars = 100 µm (A), 20 µm (B, D, F), 50 µm (C, E)*

Figure 2. Ultrastructural findings in *post-mortem* kidney biopsies from patients with COVID-19

(A, B & C) Congestion of red blood cells in peritubular capillaries and expansion of subendothelial space (C) by accumulation of an amorphous osmiophilic material; (patient #5). **(D)** Congestion in a glomerular capillary loop (patient #4); **(E & F)** Viral-likes particles corresponding to clathrin-coated vesicles in a glomerular capillary loop **(E)** and a renal cortical artery **(F)** (patient #2). *Scale bars = 5 µm (A-D), 0.1 µm (E, F)*

Figure 3. Representative serial immunostaining for CD10, 2019-nCov N protein and CD31 on *post-mortem* kidney biopsies from a patient with COVID-19

Serial sections of kidney samples from patients with COVID-19 were used for immunostaining against the proximal tubule marker, CD10 (in black) **(A)**; the 2019-nCov N protein (in red) **(B)**; and the endothelial marker, CD31 (in brown) **(C)**. A punctuate pattern for the 2019-nCov N protein is detected at the basolateral pole of CD10-negative and CD31-negative distal tubule (*) (patient #9). No specific signal is detected in CD31-positive peritubular capillaries (arrow).

Scale bars = 20 µm

Figure 4. Detection and spatial distribution of viral RNA using fluorescence *in situ* hybridization

The first (overview) and second (targeted zoom) columns display positive signal for viral RNA in different renal compartments, including proximal and distal tubules, glomeruli and vessels. nCoV2019-S RNA is in green; *Lotus tetragonolobus* lectin (LTL) is in red; DAPI is in blue (patient #4).

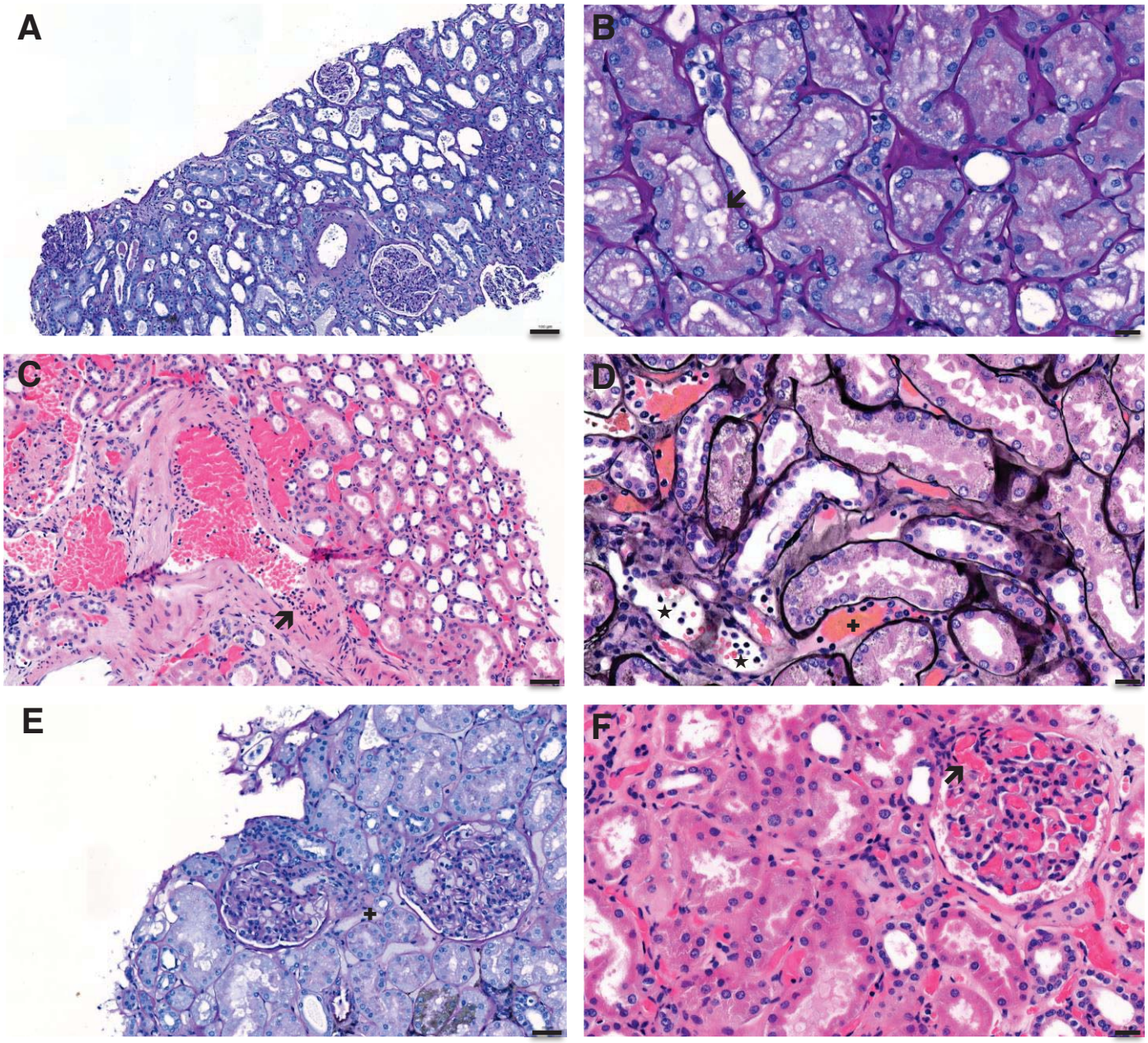

Figure 1

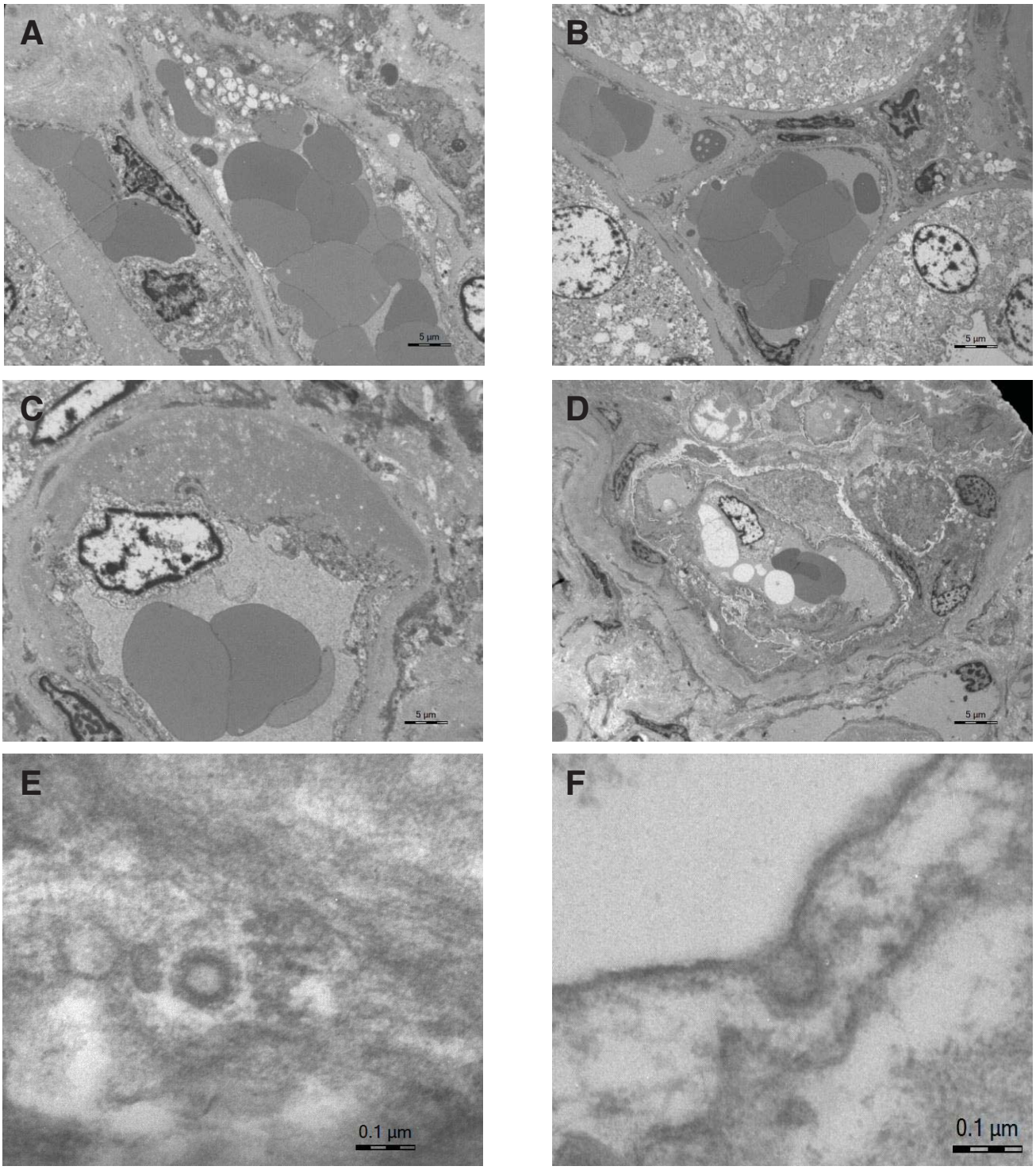

Figure 2

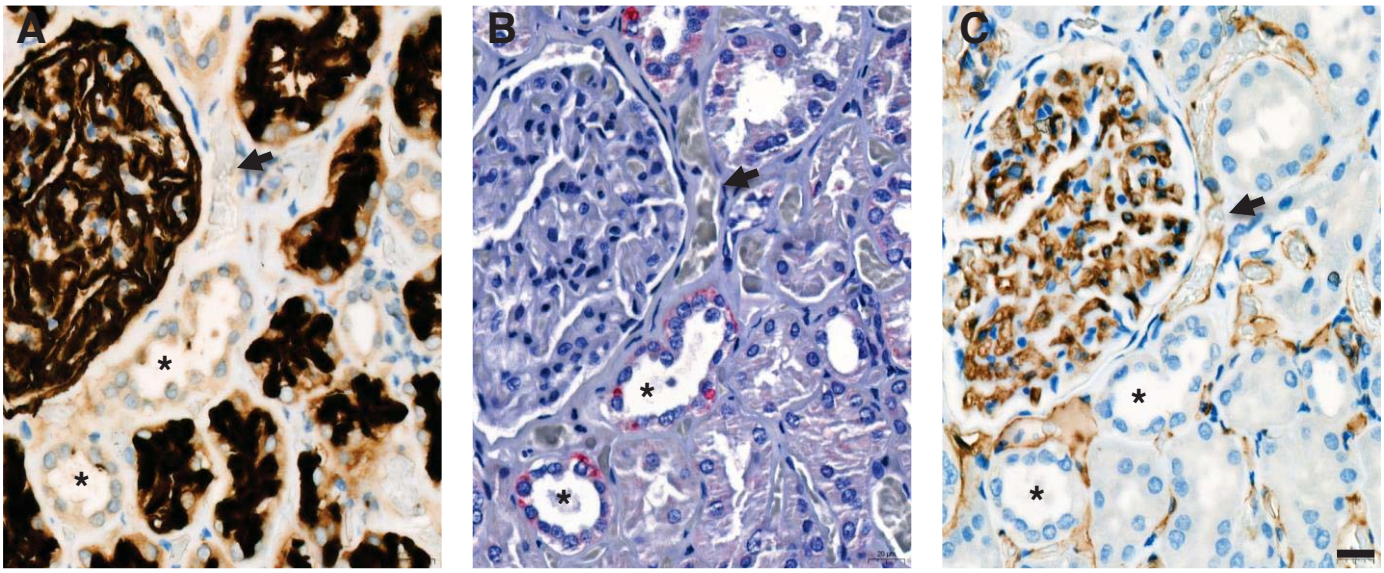

Figure 3

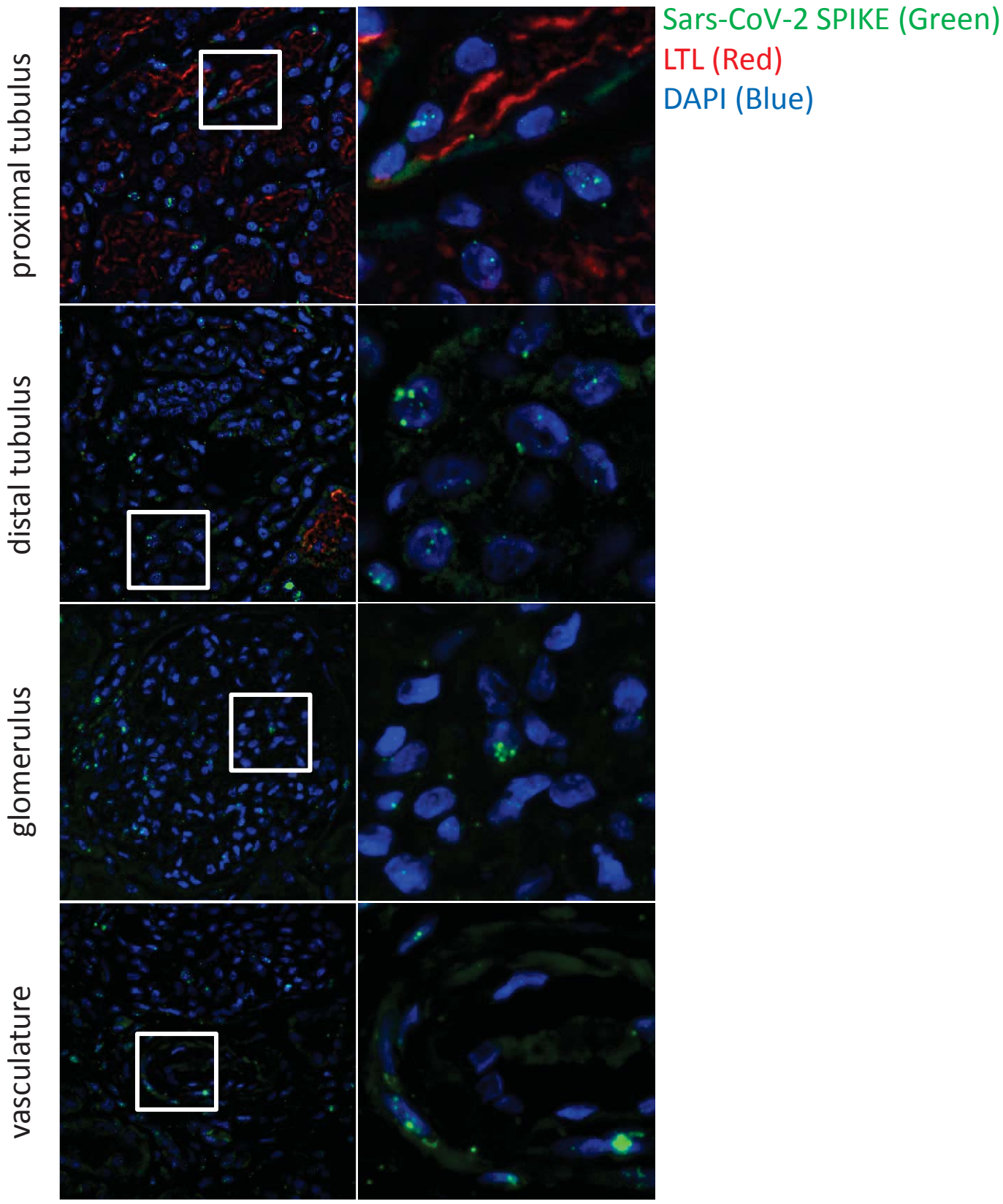
proximal tubulus
distal tubulus
glomerulus
vasculature
Sars-CoV-2 SPIKE (Green)
LTL (Red)
DAPI (Blue)

Figure 4

Supplemental Material Table of Contents

Supplementary Table 1: Criteria for the scoring of kidney samples using light microscopy

Glomerular compartment	Tubular compartment	Interstitial compartment	Vascular compartment
Glomerulosclerosis (n)	Cytoplasmic vacuolization*	Interstitial edema	***Artery***
Ischemic glomeruli	Tubular dilatation	Interstitial inflammation[$]	Arteritis[$]
Proliferative lesions	Apical blebbing	Interstitial hemorrhage	Endothelial cell swelling
- Endocapillary proliferation	Loss of brush border	Calcifications	Thrombi
- Mesangial proliferation			Vascular wall thickening
- Extracapillary proliferation	Tubular epithelium thinned	Interstitial fibrosis [$]	***Arteriole***
Mesangial matrix expansion	Necrosis		Endothelial cell swelling
FSGS lesions	Apoptosis		Thrombi
- Flocculo-capsular synechiae	***Tubular basement membrane***		Arteriolar hyalinosis[$]
- Podocyte hypertrophy	- Cell shedding		***Peritubular capillary***
- FSGS	- Diffuse denudation of the tubular basement membrane		Capillary congestion
Glomerular basement membrane	- Tubulorrhexis		Capillaritis[$]
- Splitting of GBM	Mitosis		
- Membranous glomerulopathy	***Acute tubular necrosis***		
Glomerular capillary	Predominent localization		
- Congestion	Extent*		
- Endothelial cell swelling	Severity		
- Thrombi	Intratubular pigment		
	Nuclear dystrophy		
	Viral inclusions		
	Tubular atrophy[$]		
	Tubulitis[$]		
	Renal tubular epithelial casts		
	- Hyaline		
	- Red blood cells		
	- Leukocyte		

The items are scored as present or absent, except *, scored semi-quantitatively by approximate extent of tubule involvement as: none, >0-25%, 26-50% or > 50% tubules with corresponding histological lesions and $, graded similarly to the Banff criteria[57]. FSGS: focal and segmental glomerulosclerosis; GBM: glomerular basement membrane; n: number.

Supplementary Table 2: Clinical and biological characteristics of the SARS-CoV-2-infected patients by type of hospitalization wards

	ICU wards	Non-ICU wards	p
Number of patients	10	6	
Age (years) – mean [min; max]	62 [49; 73]	78.6 [60; 95]	**0.007**
Women – (%)	30	33	ns
Body Mass index (kg/m²) – mean [min; max]	31.6 [20.7; 39.2]	29.3 [23.7; 39.6]	ns
History			
Hypertension – %	60	66.7	ns
Diabetes – %	40	83.3	ns
Chronic kidney disease – %	25	25	ns
Cancer history – %	20	0	ns
Cardiovascular disease – %	50	33.3	ns
Immunocompromise status – %	30	16.7	ns
Non-smoker – %	100	40	**0.03**
RAAS inhibitors drugs – %	60	33.3	ns
Hydroxychloroquine used – %	90	83.3	ns
Contrast products injection – %	20	16.7	ns
Anti-platelets used priori hospitalization – %	50	33.3	ns
Anticoagulation during hospitalization – %	100	33.3	**0.008**
Hospital stay length (days) – median [IQR]	22.5 [8; 45]	6 [3; 12]	**0.02**
Severity			
Thorax CT-Scanner staging			ns
Minor (<10%)	10	33.3	
Mild (10-50%)	30	50	
Severe (>50%)	60	16.7	

Renal severity			
AKI – %	80	33.3	ns
RRT initiation during hospitalization – %	30	0	ns
30% decrease of eGFR during hospitalization – %	80	0	**0.007**
Proteinuria at D0 > 500 mg/g of urine creatinine – %	50	60	ns
Hematuria at D0 – %	62.5	40	ns
Laboratory results			
ABO group – (%)			ns
A	55.6	80	
B	11.1	20	
AB	0	0	
O	33.3	0	
Lymphocytes at D0 (/mm³) – median [IQR] – (range 1100-3700/mm³)	645 [410; 1410]	990 [540; 1460]	ns
Platelets at D0 (x1000/mm³) – mean [min; max] – (range 150-353*10^3/mm^3)	183 [155; 277]	199 [137;261]	ns
CRP at D0 (mg/L) – mean [min; max] – (range 0-5mg/L)	178.6 [4.4; 382.4]	146.3 [8.5; 272.2]	ns
Fibrinogen (g/L) at D0 – median [IQR] – (range 1.79-3.86g/L)	6.58 [3.7; 7.72]	7.26 [6.31; 7.72]	ns
Procalcitonin at D0 (µg/L) – median [IQR] – (range <0.05 µg/L)	0.41 [0.14; 1.63]	0.22 [0.16; 0.53]	ns
D-Dimer at D0 (µg/L) – mean [min; max] – (range <500 µg/L)	1448.8 [565; 2991]	1142.4 [329; 2384]	ns
LDH at D0 (U/L) – mean [min; max] – (range 125-220 U/L)	618.5 [269; 881]	390 [195; 707]	ns
CPK at D0 (UI/L) – median [IQR] – (range 29-168 UI/L)	381 [240; 592]	205.5 [34; 292]	0.05
Serum creatinine at D0 (mg/L) – median [IQR] – (range 0.55-1.02mg/dL)	0.93 [072; 1.21]	1.3 [1.08; 1.57]	**0.04**
Proteinuria at D0 (mg/g of urine creatinine) – median [IQR]	595 [353; 728]	579 [303; 1104]	ns
Delay Biopsy (n=16)			ns
<60 (min) – %	60%	66.7%	
60-120 (min) – %	20%	-	
120-180 (min) – %	20%	33.3%	

AKI: acute kidney injury; COPD: chronic obstructive pulmonary disease; CPK: creatinine phospho-kinase; CRP: C-reactive protein; eGFR: estimated glomerular filtration rate; ICU: intensive care unit; IQR: interquartile range; LDH: lactate dehydrogenase; RAAS: renin angiotensin aldosterone system; RRT: renal replacement therapy; SARS-CoV-2: severe acute respiratory syndrome coronavirus 2; SD: standard deviation. p value using t-test when normally distributed variables or rank test if not normally distributed for continuous variable and Fischer exact test for categorical variables

Supplementary Table 3: Clinical and biological characteristics of the control group (SARS-CoV-2 non-infected patients)

CLINICAL	
Age (years) – mean [min; max] (n=5)	58.4 [44; 67]
Women – % (n=5)	40
Body Mass index (kg/m²) – mean [min; max] (n=4)	25.2 [16.2; 36.5]
Medical history	
Hypertension – % (n=5)	60
Diabetes – % (n=5)	20
Chronic kidney disease – % (n=5)	40
Active cancer or history – % (n=5)	40
Cardiovascular disease – % (n=5)	40
Immunocompromise status – % (n=5)	40
Non-smoker – % (n=5)	60
RAAS inhibitors drugs – % (n=5)	40
Hydroxychloroquine used – % (n=5)	0
Contrast products injection – % (n=5)	60
Anti-platelets used priori hospitalization – % (n=5)	0
Anticoagulation during hospitalization – % (n=5)	0
Hospital stay length (days) – median [IQR] (n=5)	3 [2; 17]
Severity	
ICU admission – % (n=5)	100
Renal severity	
AKI – % (n=5)	100
RRT initiation during hospitalization – % (n=5)	20
30% decrease of eGFR during hospitalization – % (n=5)	80

Proteinuria at D0 > 500 mg/g of urine creatinine – % (n=3) Hematuria at D0 – % (n=3)	66.7 100
BIOLOGICAL	
ABO group – % (n=2) A – B – AB – O	 50 – 0 – 0 – 50
Lymphocytes at D0 (/mm³) – median [IQR] (n=5)	540 [10; 1340]
Platelet at D0 (x1000/mm³) – median [IQR] (n=5) Platelet at end of hospitalization (x1000/mm³) – median [IQR] (n=5)	220 [157; 250] 129 [98; 344] †
C-reactive protein at D0 (mg/L) – median [IQR] (n=5) C-reactive protein at end of hospitalization (mg/L) – median [IQR] (n=5)	87 [41.4; 284.7] 124.8 [64; 260] †
Fibrinogen at D0 (g/L) – median [IQR]	4.1 [2.9; 6]
Procalcitonin at D0 (µg/L) – median [IQR] (n=2)	50.1 [0.11; 100]
D-Dimer at D0 (µg/L) – median [IQR] (n=3)	2196 [1050; 2400]
LDH at D0 (U/L) – median [IQR] (n=5)	294 [214; 494]
CPK at D0 (U/L) – median [IQR] (n=5)	90 [58; 149]
Serum creatinine at D0 (mg/dL) – median [IQR] (n=5) Serum creatinine at end of hospitalization (mg/dL) – median [IQR] (n=5)	1.42 [1.2; 1.63] 2.22 [1.41; 2.68] †
Potassium at D0 (mmol/L) – median [IQR] (n=5)	4.8 [4.3; 4.9]
Proteinuria at D0 (mg/g of urine creatinine) – median [IQR] (n=3)	654 [387; 2607]
Delay Biopsy (n=5) **<60 (min) – %** **>180 (min) – %**	 20 80

AKI: acute kidney injury; COPD: chronic obstructive pulmonary disease; CPK: creatinine phospho-kinase; eGFR: estimated glomerular filtration rate; ICU: intensive care unit; IQR: interquartile range; LDH: lactate dehydrogenase; RAAS: renin angiotensin aldosterone system; RRT: renal replacement therapy; SARS-CoV-2: severe acute respiratory syndrome coronavirus 2; SD: standard deviation. † no statistical difference observed between D0 and end of hospitalization

Supplementary Table 4: Cases series studies on kidney biopsies in SARS-CoV-2 infected patients

Authors (ref)	Post-mortem biopsies (n)	Clinical and biological data	Light microscopy	Immunostaining	Electron microscopy
Diao et al. (25)	Yes (n=6)	Renal dysfunction (no clear clinical or biological data) No data on delay between death and autopsy	Variable severity of ATN Lymphocytic infiltration on 5/6 biopsies	SARS-CoV-2 antigen (N protein) was detected in the renal tubules (no data on proximal or distal tubules) No ACE2 data	Virion and virus-like particles detected (2/6)
Su et al. (26)	Yes (n=26)	Either patients with AKI and no-AKI No data on delay between death and autopsy	Significant ATN Occlusion of the glomerular and peritubular capillary lumens by unfragmented erythrocytes (without evidence of thrombi, platelets or fibrinoid necrosis) No significant infiltrate	SARS-CoV-2 (N protein) was found at the nuclear or cytoplasmic level in the tubular epithelium of 3/6 patients Weak ACE2 staining of the proximal tubules (3/5)	Virion and virus-like particles detected within the epithelium of the proximal tubules, podocytes and, to a lesser extent, distal tubules (7/9)
Menter et al. (45)	Yes (n=18)	Patients with mean creatinine level of 2.8mg/dl at death Mean delay between death and autopsy was 32.9h	Diffuse ATI 3 patients showed signs of DIC with fibrin thrombi within glomerular capillaries	No data	Virus like particles in endothelial cells (2 patients)
Bradley et al. (49)	Yes (n=14)	Detailed clinical presentation with or without AKI No data on delay between death and autopsy	Mild to severe arterionephrosclerosis and diabetic nephropathy ATI (extensive tubular epithelial vacuolization) (11/14) Chronic inflammation and FSGS in 1 patient	2/10 patients with patchy, granular cytoplasmic staining of the renal tubular epithelial cells (Spike Protein)	Viral particles in tubular epithelial cells (2 patients) and more rarely in endothelial cells
Golmai et al. (50)	Yes (n=12)	Patients with AKI stage 2 or 3 but low level of proteinuria (between 30 and 100mg/dl) Delay between death and biopsy was 18.3h (2-70hours)	All patients had ATI with focal ATN, which varied from mild to diffuse No evidence of GN, vasculitis, or TMA	All biopsies showed negative immunohistochemistry staining for SARS-CoV-2 (N protein) Negative in *in situ* hybridization (4/12)	Absence of virion in renal cells (12/12)

Santoriello et al. (51)	Yes (n=42)	Detailed clinical presentation with AKI (in the majority of cases 40/42) and proteinuria (evaluated by dipstick in 23/29) 6 patients were dead at the time of admission Delay between death and autopsy was 21.8hours	All patients had ATI and arteriosclerosis No significant glomerular changes except one patient with FSGS, one with IgA nephropathy and 6 with focal (less than 5% of glomeruli) with fibrin thrombi	All biopsies showed negative immunohistochemistry staining for SARS-CoV-2 (Spike protein) (10/42) Negative in *in situ* hybridization (10/42)	No definitive virions were identified (8/42)
Xia et al.	Yes (n=10)	Detailed clinical and biological presentation with AKI (in all cases 10/10) and low level of proteinuria (evaluated by dipstick) No data on delay between death and autopsy	All patients showed various degree of ATI Glomerular lesions were not remarkable except swollen endothelial cells Venous thrombosis in a patient with anti-phospholipid antibodies	All biopsies showed negative immunohistochemistry staining for SARS-CoV-2 (Spike protein) RNA extraction of SARS-CoV-2 (N-gen) from kidney samples all negative (9/10)	A few particles of a diameter of about 60–100 nm were observed in the cytoplasm of renal proximal tubular epithelial cells and some of these particles were enclosed in vesicles
Sharma et al. (48)	No (n=10)	All with various level of AKI (8/10 on RRT) and proteinuria with or without hematuria	Various level of ATN in all patients TMA (2/10) FSGS (1/10)	All biopsies showed negative immunohistochemistry staining for SARS-CoV-2 (N protein)	No evidence of viral presence
Kudose et al.	No (n=17)	Various level of AKI (15/17) and proteinuria (9/17 nephrotic range) with or without hematuria	Various level of ATI in all patients FSGS (5/17) MCD (1/17) Tubulo-reticular inclusions (2/17) MN (2/17) Lupus nephritis (1/17) Anti-GBM (1/17) Cellular rejection (for transplanted patients 3/17)	No definitive staining (16/17) (Spike Protein) Possibly positive tubular cell staining in 2 cases in *in situ* hybridization (2/16)	Absence of virion in renal cells (13/17)
Akilesh et al.	No (n=17)	Detailed clinical and biological presentation with AKI (in all cases 15/17) and proteinuria (11/17)	ATI within 13/17 patients FSGS within 11/17 patients MCD within 1/17 patients Acute endothelial cells injury within 6patients	4/17 biopsies showed negative immunohistochemistry staining for SARS-CoV-2 (N protein) Negative in *in situ* hybridization (4/17)	No definitive virions were identified (17/17)

Nasr et al.	No (n=13)	Detailed clinical and biological presentation with AKI (in all cases 13/17) and proteinuria (11/13)	Diffuse ATI (13/13) Collapsing glomerulopathy (8/13) MN (1/13) RPGN (1/13) Diabetic glomerulosclerosis (3/13) Pre-existing known condition in 3/13 (MN, IgA nephropathy and diabetic nephropathy)	Negative in *in situ* hybridization (1/13)	No definitive virions were identified (13/13)
Shetty et al. (46)	No (n=6)	Detailed clinical and biological presentation with AKI in all cases and proteinuria in all case (4 native kidney and 1 kidney transplant patient, 2 patients with CKD previously to admission)	Collapsing glomerulopathy (5/6) Diabetic glomerulosclerosis (1/6)	Not done	No definitive virions were identified (6/6)

ACE2: angiotensin-converting enzyme 2; AKI: acute kidney injury; ATI: acute tubular injury; ATN: acute tubular necrosis; CKD: chronic kidney disease; DIC: disseminated intravascular coagulation; FSGS: focal segmental glomerulosclerosis; GBM: glomerular basement membrane; GN: glomerulonephritis; MN: membranous nephropathy; MCD: minimal change disease; NP: nucleocapsid protein; RNA: ribonucleic acid; RPGN: rapidly progressive glomerulonephritis; RRT: renal replacement therapy; SARS-CoV-2: severe acute respiratory syndrome coronavirus 2; TMA: thrombotic micro-angiopathy.

Supplementary Figure 1. Non-thrombotic congestion in glomerular and peritubular capillaries of kidney samples from patients with COVID-19

(A) Hematoxylin & Eosine coloration; (B) Immunostaining against the platelet marker, CD42; (C) Immunostaining against the platelet marker, CD61; (D) Martius Blue Scarlett staining. (patient #6). *Scale bar, 50 µm.*

Supplementary Figure 2. Representative immunostaining for angiotensin-converting enzyme 2 (ACE2) in post-mortem paraffin-embedded kidney tissue from a patient with COVID-19 (patient #11)

ACE2 mainly stained the brush border of proximal tubules with a weak cytoplasm staining. A segmental and focal staining of glomerular parietal epithelial cells is also observed.

Supplementary Figure 3. Positive immunohistochemistry staining for the SARS-CoV-2 nucleocapsid protein at low power magnification

IHC staining of renal biopsy tissue from two different patients with COVID-19 (A,B patient #3) and (C,D patient #1) shows positivity in some tubules. Higher magnification for the boxed area with scale bars = 100 µm (A,C) and 50 µm (B,D)

Supplementary Figure 4. Immunostaining for (A) nucleocapsid protein of the SARS-CoV-2 (NP) and (B) Sodium-Chloride cotransporter (NCC) on serial paraffin-embedded sections

Some NCC-positive tubes (symbols) demonstrate non-uniform positivity for nucleocapsid protein of the SARS-CoV-2 (patient #6). *Scale bars: 20 µm (A,B).*

Supplementary Figure 5. Detection and spatial distribution of viral RNA using fluorescence *in situ* hybridization.

nCoV2019-S RNA is in green; *Lotus tetragonolobus* lectin (LTL) is in red; DAPI is in blue (patient #2, patient #4).

Supplementary Figure 6. Experimental controls of the fluorescent *in situ hybridization* experiment

The column on the left displays positive signal for the housekeeping genes UBC (Polyubiquitin-C) and PPIB (Peptidyl-prolyl cis-trans isomerase B) in patients #2 and #10, whereas the column on the right shows negative signal (with a negligible level of background) for the bacterial dapB.

Supplementary Figure 7. Experimental controls of the immunostaining procedures

Representative images of negative (kidney sample from control #P1 patient) (A) and positive (lung sample of a guinea pig infected by SARS-Cov-2) (B) cases of immunostaining for the nucleocapsid of SARS-CoV-2 using 2019-nCoV N-Protein (NP) rabbit polyclonal antibody (ABclonal #A20016). *Scale bars: 200 µm (A), 100 µm (B).*

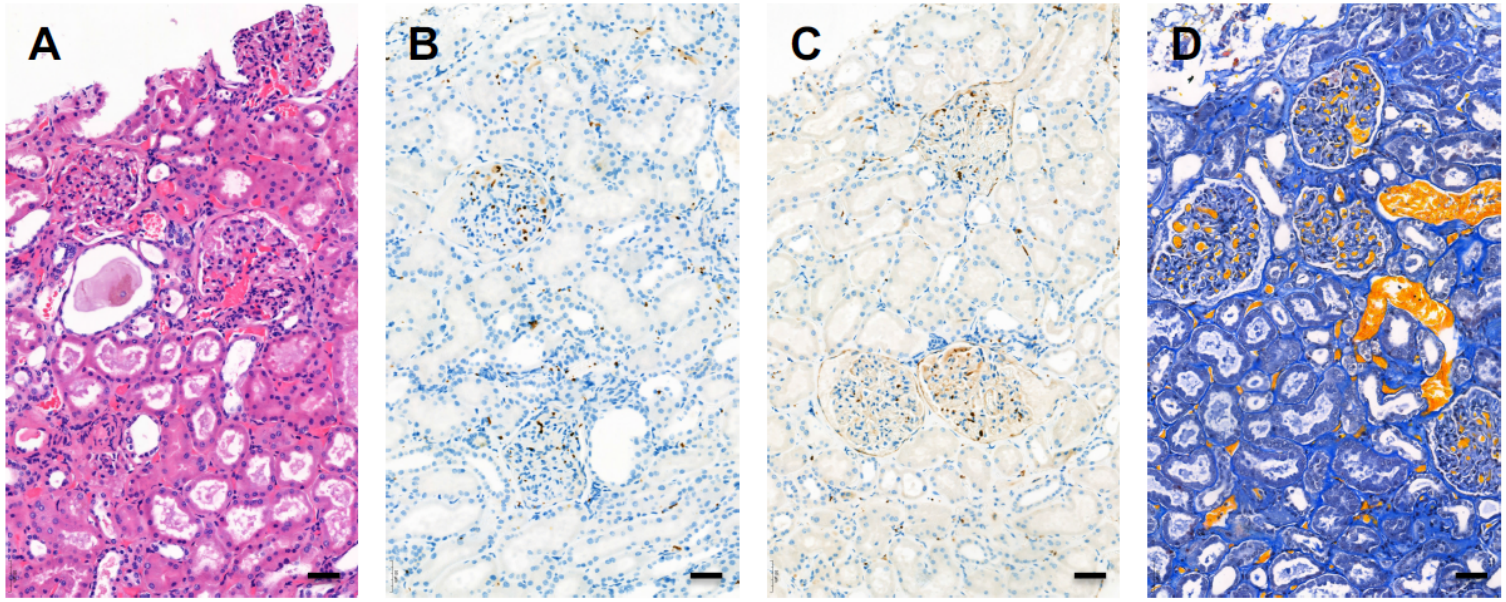

Supplementary Figure 1

A

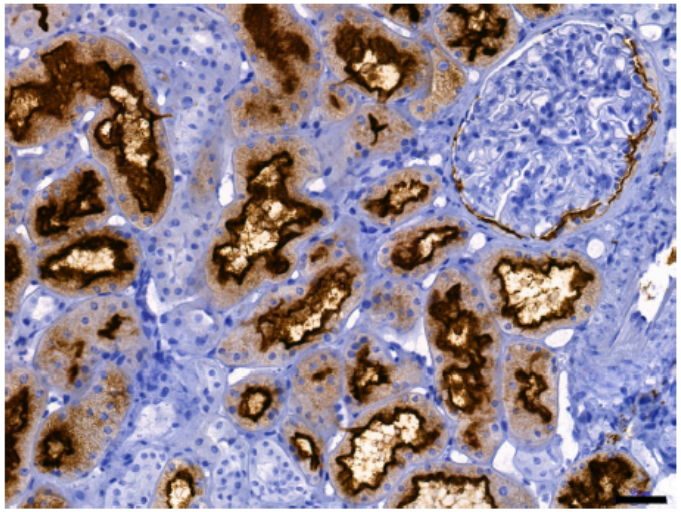

Supplementary Figure 2

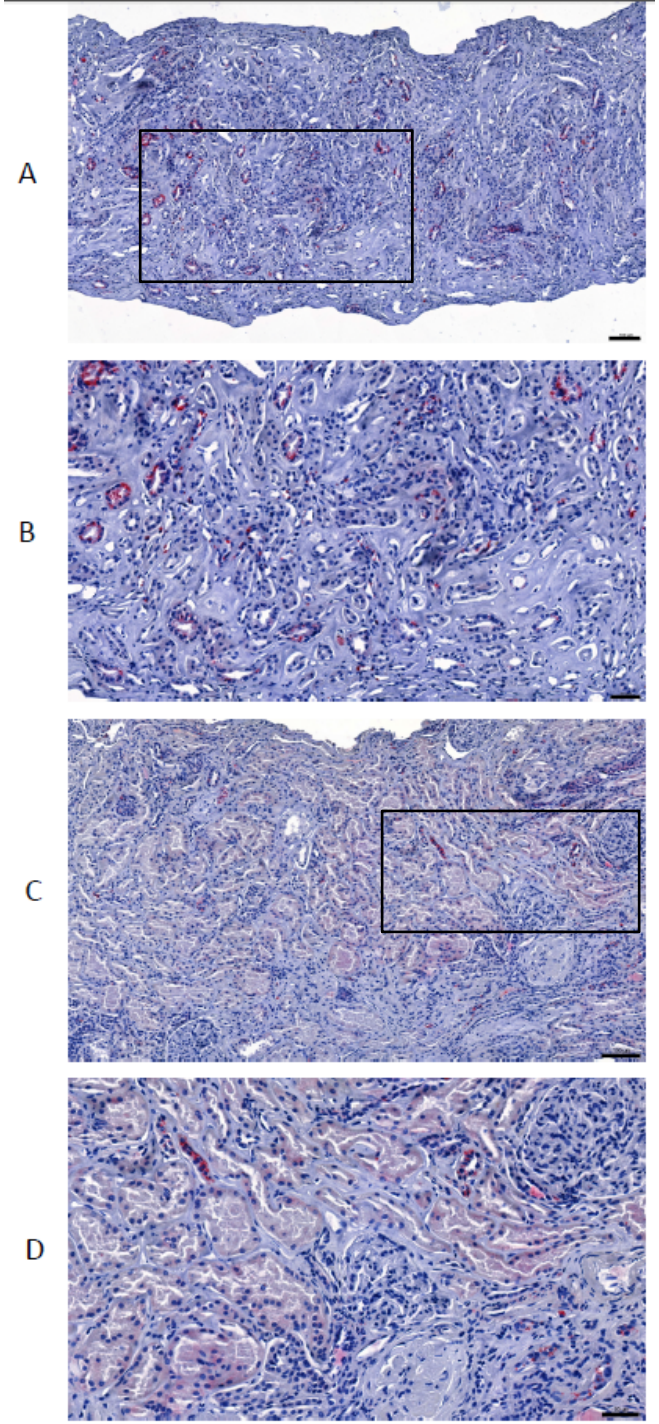

Supplementary Figure 3

A

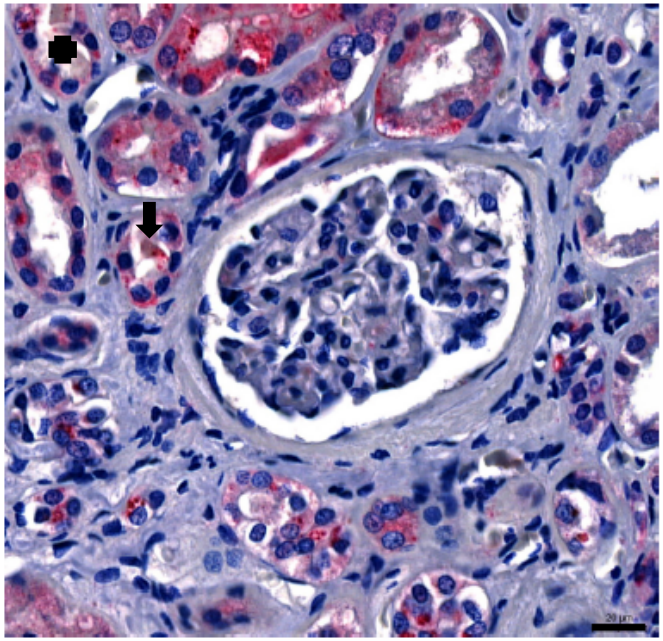

B

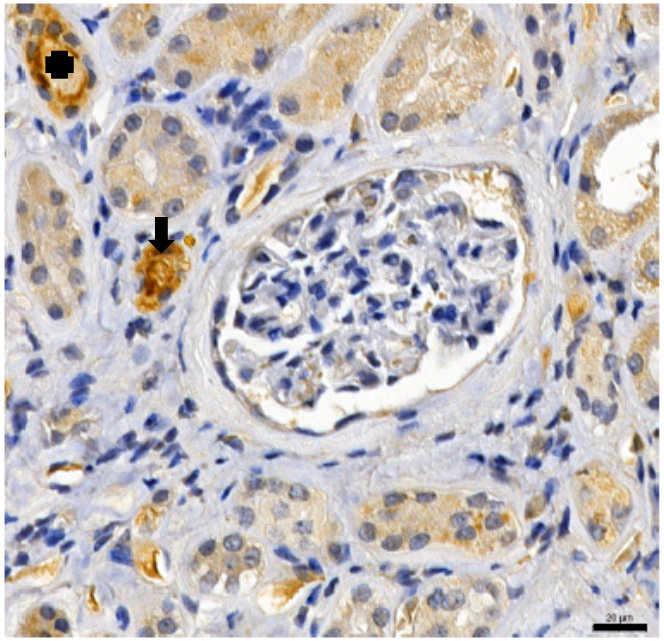

Supplementary Figure 4

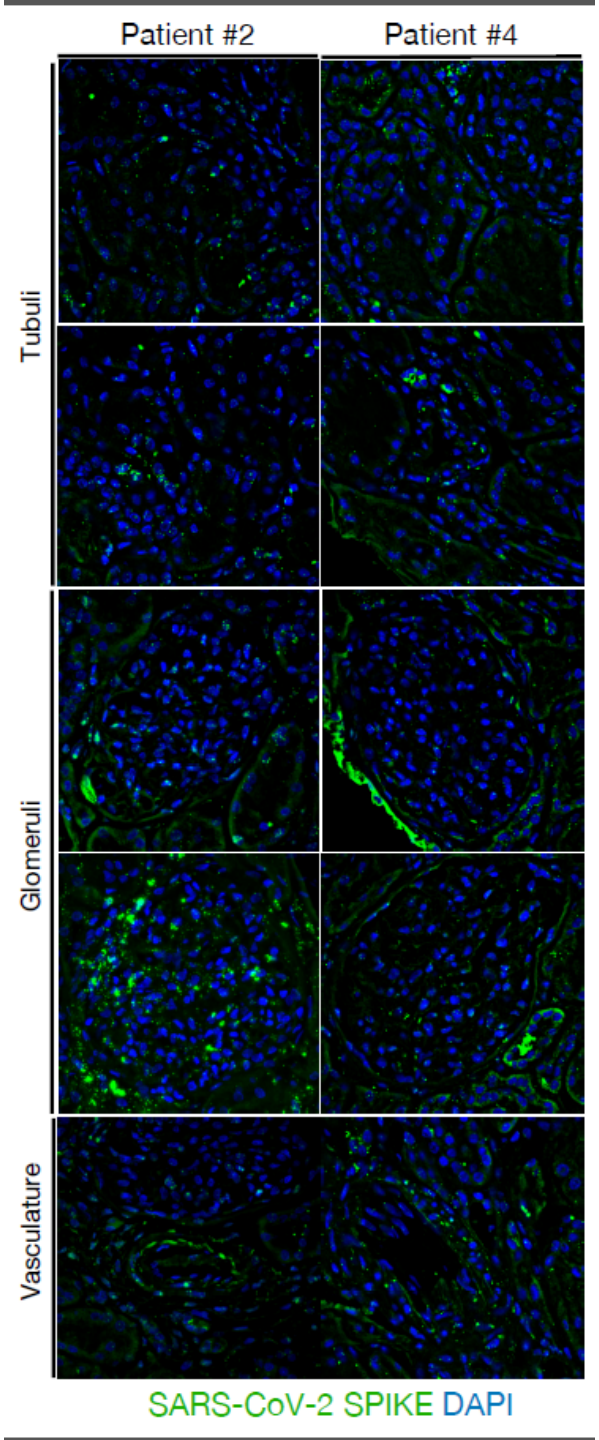

Supplementary Figure 5

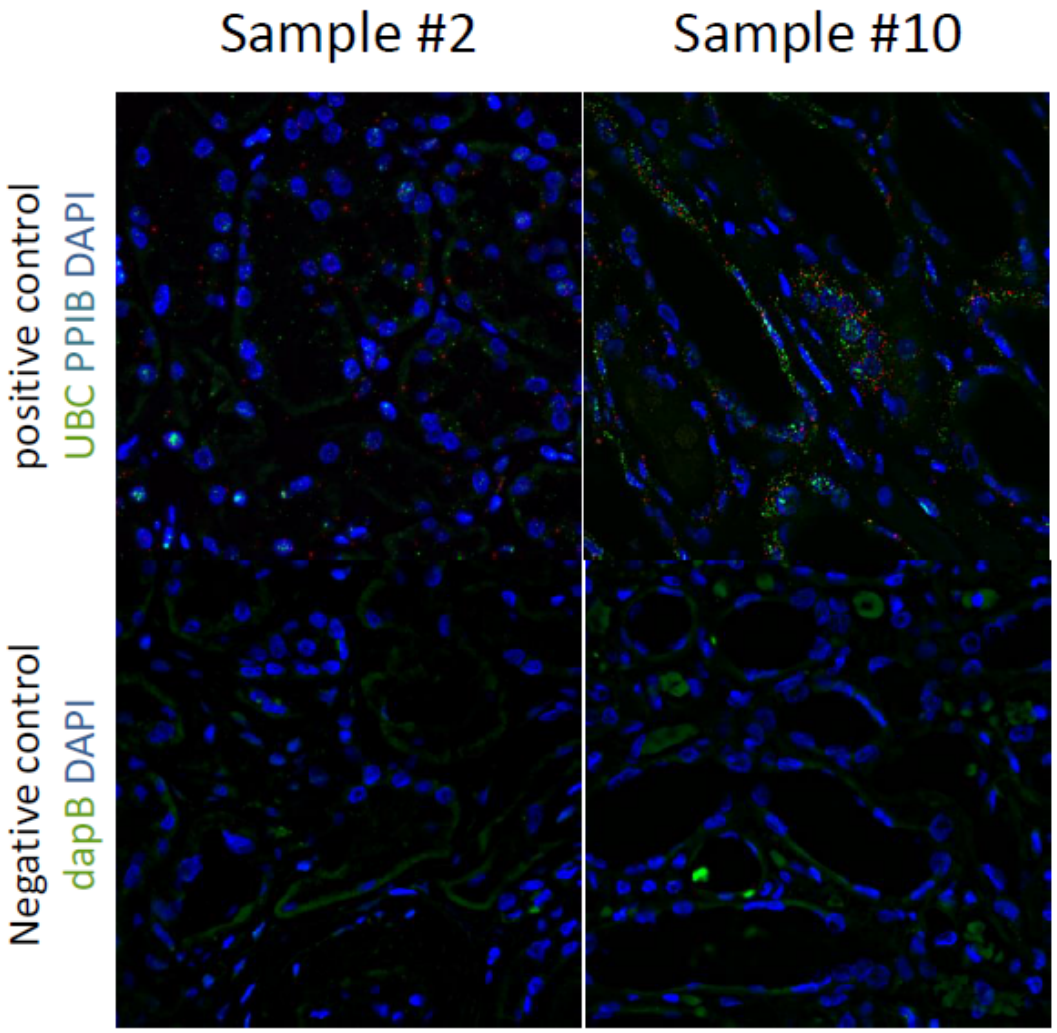

Supplementary Figure 6

A

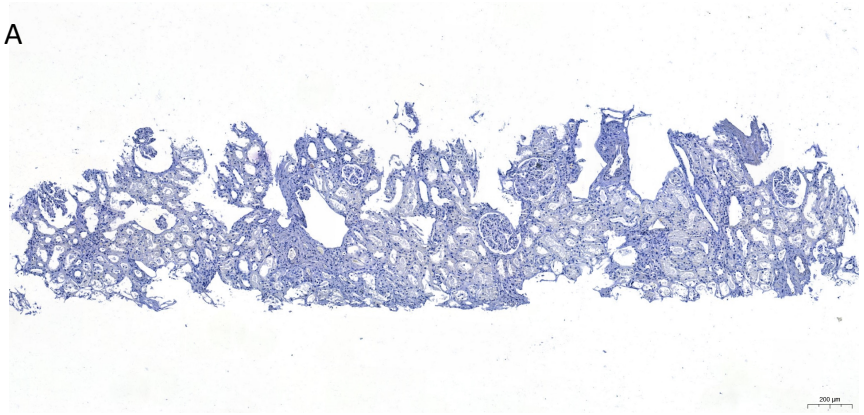

B

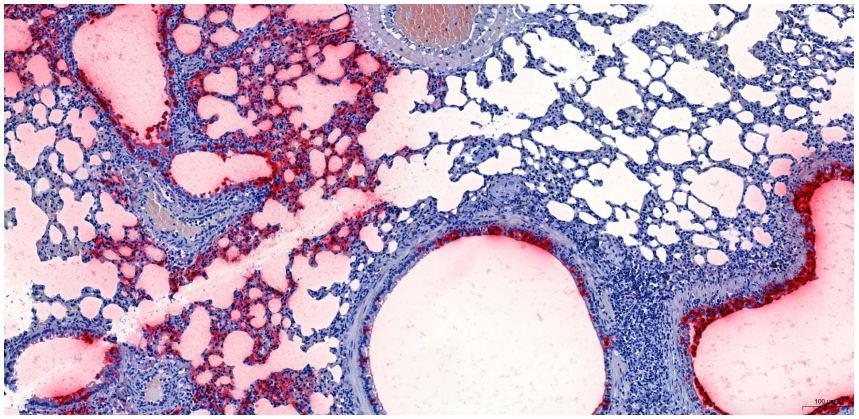

Supplementary Figure 7